

SUPPORTING INFORMATION

Divergent Structure-Activity Relationships of Structurally Similar Acetylcholinesterase Inhibitors

C. David Andersson,[#] Nina Forsgren,[□] Christine Akfur,[□] Anders Allgardsson,[□] Lotta Berg,[#] Cecilia Engdahl,^{#,□} Weixing Qian,[#] Fredrik Ekström,^{□,*} and Anna Linusson.^{#,*}

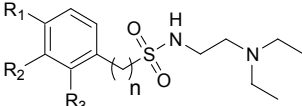
[#] Department of Chemistry, Umeå University, SE-901 87 Umeå, Sweden. [□] Swedish Defense Research Agency, CBRN Defense and Security, SE-906 21 Umeå, Sweden.

Contents

S2-S3	Bioassay results of compound sets 1 and 2
S4-S7	ITC heat-diagrams and titration curve-fitting
S8	Crystallographic data collection and refinement statistics
S9-S12	General description of the crystal structures and key protein-ligand interactions
S13-S15	Structural comparisons of benzylic and non-benzylic inhibitors with donepezil and HI-6
S16-S38	¹ H- and ¹³ C NMR-spectra
S39-S46	Analytical HPLC spectra
S47	References

Bioassay results of compound sets 1 and 2

Table S2. Compound inhibition of AChE hydrolysis of Set 1.

Compound					Bioreplicate A		Bioreplicate B		
	ID (name)	n	R1	R2	R3	IC_{50} (μ M)	95 % CI (μ M) ^a	IC_{50} (μ M)	95 % CI (μ M) ^a
2 (AL029)	1	H	H	H	H	128	118 - 140	139	122 - 158
3 (AL032)	1	CH ₃	H	H	H	52	47 - 58	49	41 - 58
4 (AL036)	1	F	H	H	H	44	29 - 66	40	34 - 46
5 (AL011)	1	Cl	H	H	H	16	13 - 19	12	11 - 13
6 (AL037)	1	CF ₃	H	H	H	22	19-25	12	10-14
7 (AL038)	1	Br	H	H	H	11	10-13	10	9-11
8 (AL031)	1	Cl	Cl	H	H	6	5 - 7	7	6 - 8
9 (AL039)	0	H	H	H	H	34	26 - 44	31	27 - 36
10 (AL034)	0	H	H	F	H	43	38 - 49	41	36 - 46
11 (AL041)	0	H	OCH ₃	H	H	13	11 - 15	7	6 - 8
12 (AL040)	0	H	CF ₃	H	H	27	21 - 33	22	19 - 24
13 (AL024)	0	H	Cl	H	H	21	18-23	18	15-20
14 (AL027)	0	OCH ₃	H	H	H	118	96 - 146	119	97 - 145
15 (AL025)	0	CH ₃	H	H	H	136	121 - 153	135	117 - 156
16 (AL033)	0	F	H	H	H	69	63 - 75	62	54 - 70
17 (AL028)	0	Cl	H	H	H	93	73 - 119	88	74 - 106
18 (AL026)	0	NO ₂	H	H	H	103	90 - 117	95	81 - 111
19 (AL030)	0	Cl	H	F	H	96	83 - 113	91	80 - 103
20 (AL023)	0	F	F	H	H	52	46 - 60	50	40 - 63

^a 95% confidence intervals calculated from at least four replicates.

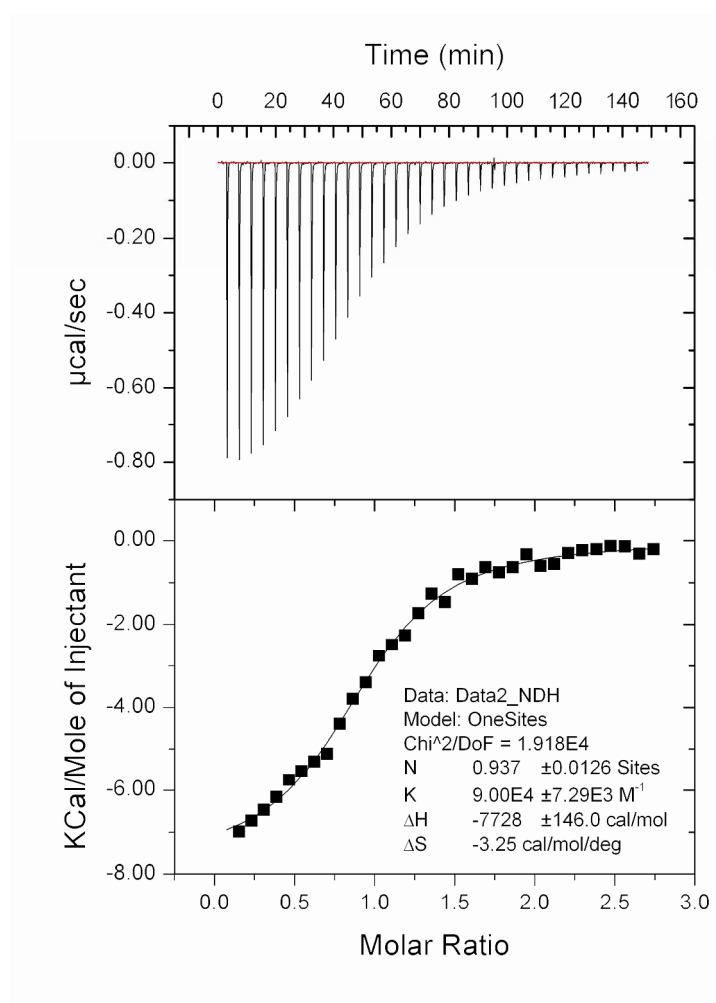
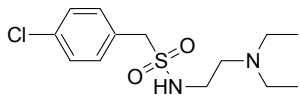
Table S3. Compound inhibition of AChE hydrolysis of Set 2.

Compound	ID (name)	R	Bioreplicate C ₁		Bioreplicate C ₂	
			IC ₅₀ (μM)	95 % CI (μM) ^a	IC ₅₀ (μM)	95 % CI (μM) ^a
21 (AL144)			44	32-58	37	25-54
22 (AL143)			>700		NA ^b	
23 (AL149)			>700		NA ^b	
24 (AL151)			2.5	2.3-2.8	2.4	2.3-2.7

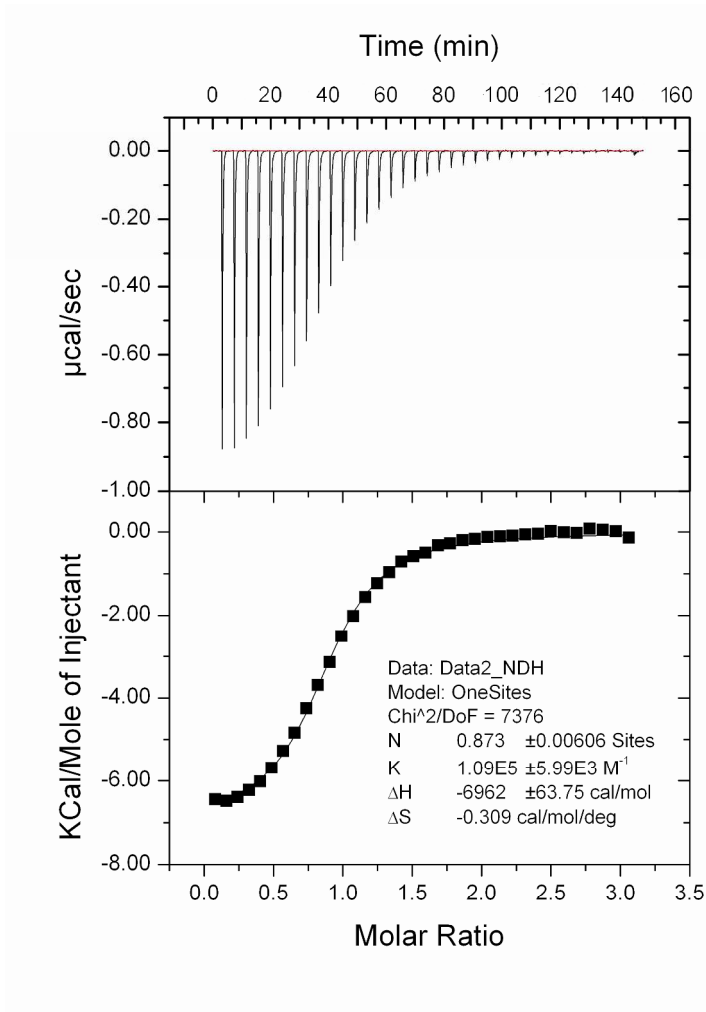
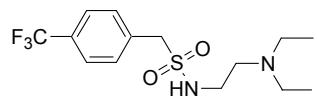
^a 95% confidence intervals calculated from at least four replicates. ^b Not analyzed.

ITC heat-diagrams and titration curve-fitting

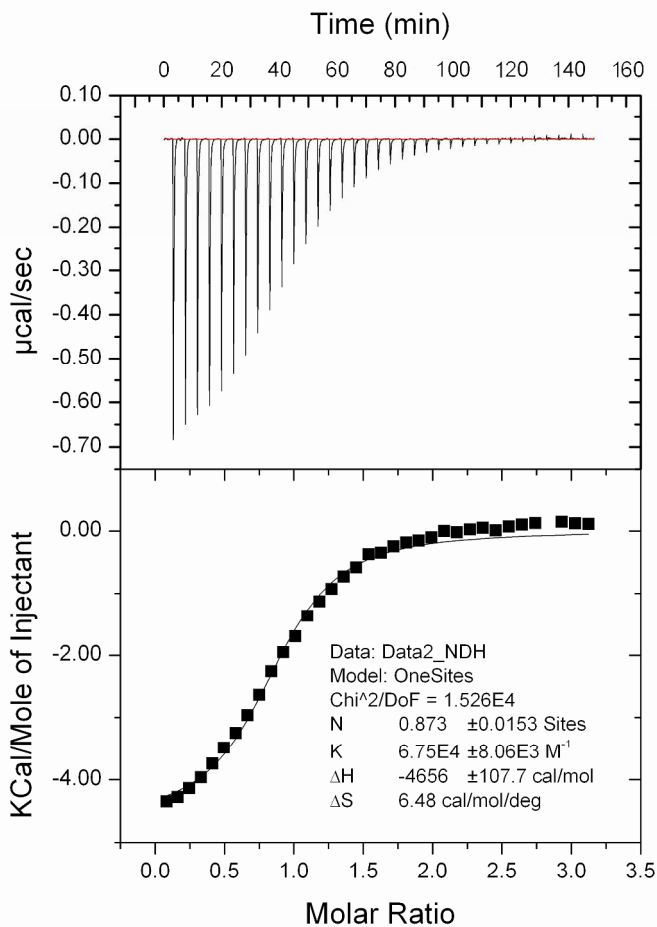
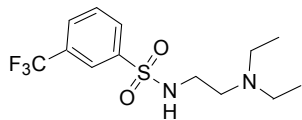
5 (AL011)



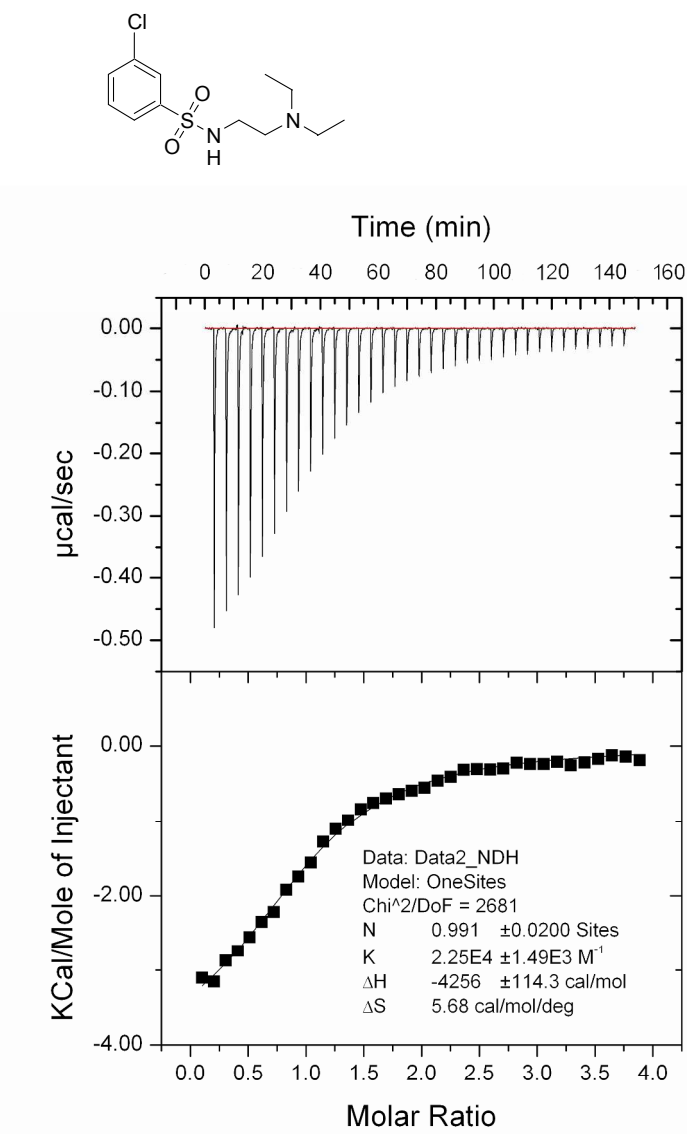
6 (AL037)



12 (AL040)



13 (AL024)



Crystallographic data collection and refinement statistics

Table S8. Crystallographic Data Collection and Refinement Statistics

	3 (AL032)	4 (AL036)	5 (AL011)	10 (AL034)	11 (AL041)	12 (AL040)	17 (AL028)	24 (AL151)
Data collection								
PDB entry code	4b7z	4b80	4b81	4b82	4b83	4b84	4b85	4bt1
Wavelength (Å)	1.039	1.041	1.039	1.039	1.041	1.041	1.0	0.981
Space group	P2 ₁ 2 ₁ 2 ₁							
Unit cell (Å)	79.3 x 111.8 x 226.7	78.9 x 111.5 x 227.6	78.0 x 109.9 x 227.9	80.5 x 111.9 x 226.9	79.6 x 111.9 x 227.8	79.1 x 112.4 x 227.2	79.5 x 112.9 x 226.5	78.7 x 110.8 x 227.1
Resolution (Å)	29.12-2.3 (2.42-2.30)	29.01-2.5 (2.64-2.50)	29.3-2.80 (2.95-2.80)	29.19 -2.1 (2.21-2.10)	29.22-2.40 (2.53-2.40)	29.75-2.60 (2.74-2.60)	29.2-2.10 (2.21-2.10)	29.05-2.50 (2.64-2.50)
No. of reflections	537639 (16744)	320717 (46534)	199177 (28373)	585288 (81250)	598212 (85602)	286748 (41247)	693887 (99375)	445633 (64698)
Unique reflections	90383 (13047)	70343 (10146)	49067 (7029)	120032 (17282)	80333 (11581)	57324 (8499)	119406 (17273)	69367 (10003)
Completeness (%)	99.9 (99.7)	99.9 (100)	99.9 (100.0)	99.5 (98.0)	99.9 (100)	91.5 (93.6)	99.8 (99.8)	99.7 (99.6)
Multiplicity/Redundancy	5.9 (5.8)	4.6 (4.6)	4.1 (4.0)	4.9 (4.7)	7.4 (7.4)	5.0 (4.9)	5.8 (5.8)	6.4 (6.5)
R _{merge} ^a	0.067 (0.497)	0.088 (0.663)	0.089 (0.525)	0.049 (0.405)	0.069 (0.575)	0.071 (0.0481)	0.054 (0.417)	0.077 (0.452)
(I)/σ(I)	16.9 (4.3)	14.6 (2.7)	13.7 (2.8)	22.1 (4.7)	20.5 (4.3)	17.0 (3.5)	18.7 (4.5)	13.7 (3.4)
Refinement								
R-factor ^b /R _{free} ^c (%)	17.1/20.1	18.7/22.3	19.7/23.9	19.1/21.5	19.3/22.2	17.6/23.6	17.7/20.6	19.1/23.2
RMS bonds (Å)	0.008	0.008	0.005	0.004	0.007	0.009	0.008	0.007
RMS angles (°)	1.086	1.082	0.920	0.900	1.074	1.212	1.119	1.094
Ramachandran plot %/no. of residues								
Favored	97.3	96.7	95.4	97.3	97.2	95.5	96.6	96.7
Allowed	2.4	3.2	4.3	2.5	2.7	4.1	3.1	2.9
Outlier	0.4	0.1	0.3	0.2	0.1	0.4	0.4	0.4

^aR_{merge} = $(\sum|I - \langle I \rangle|) / \sum I$, where I is the observed intensity and $\langle I \rangle$ is the average intensity obtained after multiple observations of symmetry related reflections.

^bR-factor = $(\sum |F_o - F_c|) / \sum F_o$, where F_o are observed and F_c calculated structure factors.

^cR_{free} uses 2% randomly chosen reflections defined in Brunger.¹

General description of the crystal structures and key protein-ligand interactions

The overall structure of the eight crystal structures is very similar to the *apo* structure of *mAChE* (PDB entry code: 1J06)² with no evident major structural changes to the protein backbone and a main chain root-mean-square deviation (rmsd) ranging between 0.19 Å and 0.28 Å for the different complexes. Similar to other *mAChE* structures, the electron density in the loop region around residue 497 is disordered, resulting in a few outliers in the Ramachandran plot (Table S8). In addition, most of the residues within the loop region around residue 258-264 could not be modeled from the acquired data. The electron density maps convincingly define the interaction patterns for the ligands with exception of compound **17** that shows signs of a conformational mobility (discussed below). Moreover, the general binding poses of the different benzenesulfonamides and benzenemethanesulfonamides are very similar, particularly within the CAS region. In general, the diethyl-amine is at contact distance to the indole ring of Trp86, the linker extends towards Phe338 and Tyr337 and the sulfonamide oxygens face Gly122 and Ser203. In the PAS region, the benzene ring system is directed towards Tyr341, forming either an edge-to-face (non-benzylic subgroup); a face-to-face interaction (benzylic subgroup); or showing signs of a high mobility (compound **17**).

Focusing on the CAS interaction of the ligands, the diethyl-amine can adopt two distinct interinversions; either exposing the nitrogen lone pair electrons (or hydrogen if protonated) to the indole ring of Trp86, or forming an intramolecular hydrogen bond with one of the sulfonamide oxygens. The intramolecular hydrogen bond results in a conformation that shields the cationic nitrogen from the aromatic system. To investigate which interinversion type that dominates, we carefully examined the simulated annealing omit electron density maps of the structures of highest resolution. At the intermediate resolution of the structural data, it is challenging to unambiguously distinguish between the two alternatives. However, we deem that the electron density maps favor the interinversion that allows for an intramolecular hydrogen bond, and the structures were refined accordingly. The conserved water molecule (WAT 1098) coordinated by Glu202 in the *apo* structure of *mAChE* is not found in this set of structures. Instead, the

side chain of Glu202 is found at contact distance to one of the ethyl groups of the diethyl-amine moiety. The electron density maps indicate that a water molecule bridges the interaction between one of the sulfonamide oxygens and Ser203Oy (the water molecule is included in the structures of compound **3**, **5**, **10**, **11**, **17**). The distances of this interaction is 2.08-3.06 Å (between Ser203Oy and the oxygen atom of the water molecule) and 2.38-3.23 Å (between the oxygen atom of the water molecule and the sulfonamide oxygen).

The main structural differences between the benzylic and non-benzylic subgroups are found within the PAS region. The benzylic subset (*i.e.* **3**, **4** and **5**) has ligands that are well resolved in the electron density maps. This set of structures is structurally similar with the ligands adapting nearly identical poses. The aromatic system of the ligands extends towards the phenyl ring of Tyr341 forming an interaction of the parallel-displaced face-to-face type. Additional main contacts (distance < 4 Å) are found to the side chains of Asp74, Tyr124, Trp286, Phe338 and Phe297.

The aromatic system of the non-benzylic subset of compounds (*i.e.* **10**, **11**, **12**, and **17**) extends towards the side chain of Tyr341 and **10**, **11**, and **12** forms an edge-to-face interaction with the phenyl ring. Additional main contacts are found with the side chains of Tyr124, Tyr337, Phe338 and Phe297. Compared to the benzylic subset, the non-benzylic compounds show a higher degree of structural variation. For example, compound **10** has two conformers of the aromatic system, related *via* a two-fold rotational axis coinciding with the sulfur-benzene bond. Moreover, the electron density map of **17** is disordered, suggesting a high degree of conformational mobility. **The benzene ring is represented as two conformers in chain A and a third conformation in chain B; the electron density maps suggest that the aromatic system has an assembly of conformations.** The conformational mobility is likely caused by a steric clash between the *para*-substituted ring system of **17** and the side chain of Tyr341. The steric clash forces **17** to adjust to alternative conformations, thereby also affecting the conformation of the Phe338 side chain.

The benzene ring of the bicyclic aromatic system of compound **24** extends towards the side chain of Tyr341 in the same manner as the other non-benzylic inhibitors. The ether-linked 2-chloro-5-nitrobenzene of **24** is involved in a face-to-face stacking interaction with Trp286.

An area with excessive electron density is found in the upper PAS region, at the entrance of the active site gorge (*i.e.* around the side chains of Tyr71, Asp74, Tyr341 and Trp286). No ligand was modeled in the structures of **11**, **12** and **17**; in the structures of **3** and **4** a poly-ethylene-glycol ligand was modeled; and in the structures of **3**, **5**, and **10**, water molecules were included in the final model. In the structure of *mAChE*•**24**, this electron density clearly defines an additional ligand as well as a poly-ethylene-glycol ligand. Interestingly, a strong density feature was found close to Pro25. Modeling this density as a sulfate ion gives a good correlation to the electron density maps. Additional density in this area suggests that the site may actually bind the ligands. Secondary ligand sites are also implicated by excessive density close to Arg219 (visible in the structures of **3**, **10**, **11**, **12** and **17**, ligand included in *mAChE*•**11**) and close to Glu81 (visible in all structures, ligand included in *mAChE*•**12**). Noteworthy, is that the ligand concentration during the soaking experiments is very high. The biological significance of secondary sites, such as the additional ligand modeled in *mAChE*•**24**, remains to be investigated although the biochemical and the thermodynamic assays showed a 1:1 ratio between ligands and AChE within the assayed concentration ranges.

Table S12. Distances between inhibitors and key amino acids in AChE.

Compound	chain	Protein	Distances (Å)					
			Trp86–		Tyr124–		Tyr124	Trp286–
			N-C ^a	Ethyl	Tyr341–	sulfon-	Phe338–	OH-
				phenyl ^b		amide ^c	phenyl ^b	phenyl ^d
3 (AL032)	A		3.9	4.2 (face-to-face)		3.7 (S=O)	-	3.1
4 (AL036)	A		3.7	4.2 (face-to-face)		3.5 (S-N)	-	3.3
5 (AL011)	A		3.9	4.4 (face-to-face)		3.2 (S=O)	-	3.0
10 (AL034)	A		3.7	4.7 (edge-to-face)		3.4 (S=O)	-	-
11 (AL041)	A		3.7	4.7 (edge-to-face)		3.4 (S-N)	4.4 (face-to-face)	-
12 (AL040)	A		3.8	4.6 (edge-to-face)		3.6 (S-N)	4.9 (face-to-face)	-
17 (AL028)	A		3.7	-		3.9 (S-N)	4.4 (face-to-face)	-
17 (AL028)	B		4.1	5.4 (edge-to-face)		4.2 (S=O)	4.6 (edge-to-face)	-
24 (AL151)	A		3.9	-		-	4.7 (face-to-face)	-
								4.0(face-to-face)

^a Distance of inhibitor ethyl amine carbon closest to Trp86 benzene centroid. ^b Inhibitor phenyl centroid to amino acid phenyl centroid. ^c Heavy atom distance between Tyr124 hydroxyl and inhibitor sulfonamide oxygen or nitrogen. ^d Heavy atom distance between Tyr124 hydroxyl and inhibitor phenyl centroid.

Structural comparisons of benzylic and non-benzylic inhibitors with donepezil and HI-6

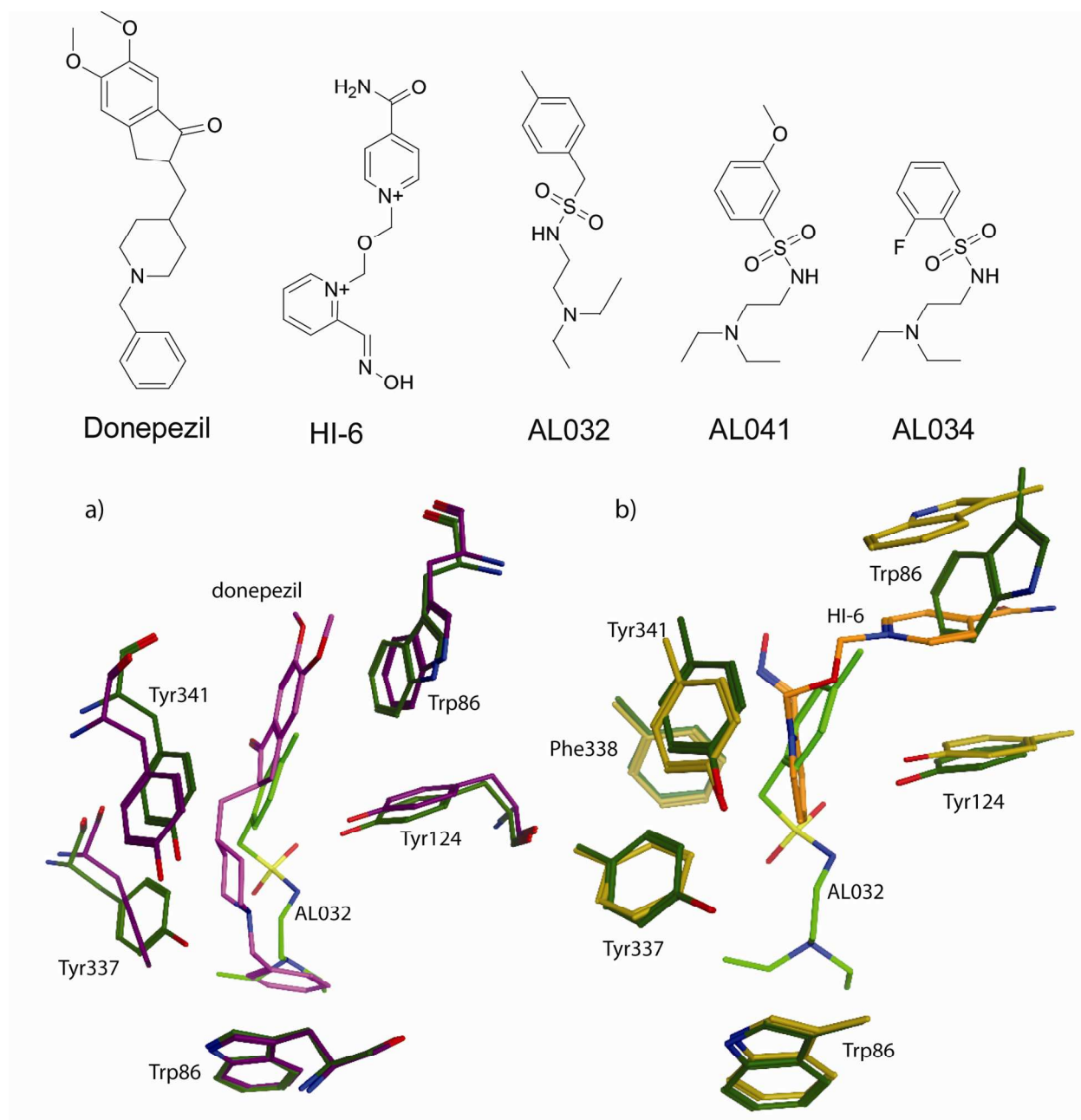


Figure S13. AChE•3 (AL032) (green, *m*AChE numbering) superposed (C_{α} -carbons) with the MOE software³ on a) AChE•donepezil (purple) crystal structure (PDB code 1EVE,⁴ *Torpedo californica* AChE), and b) AChE•HI-6 (yellow/orange, PDB code 2GYU), *m*AChE .

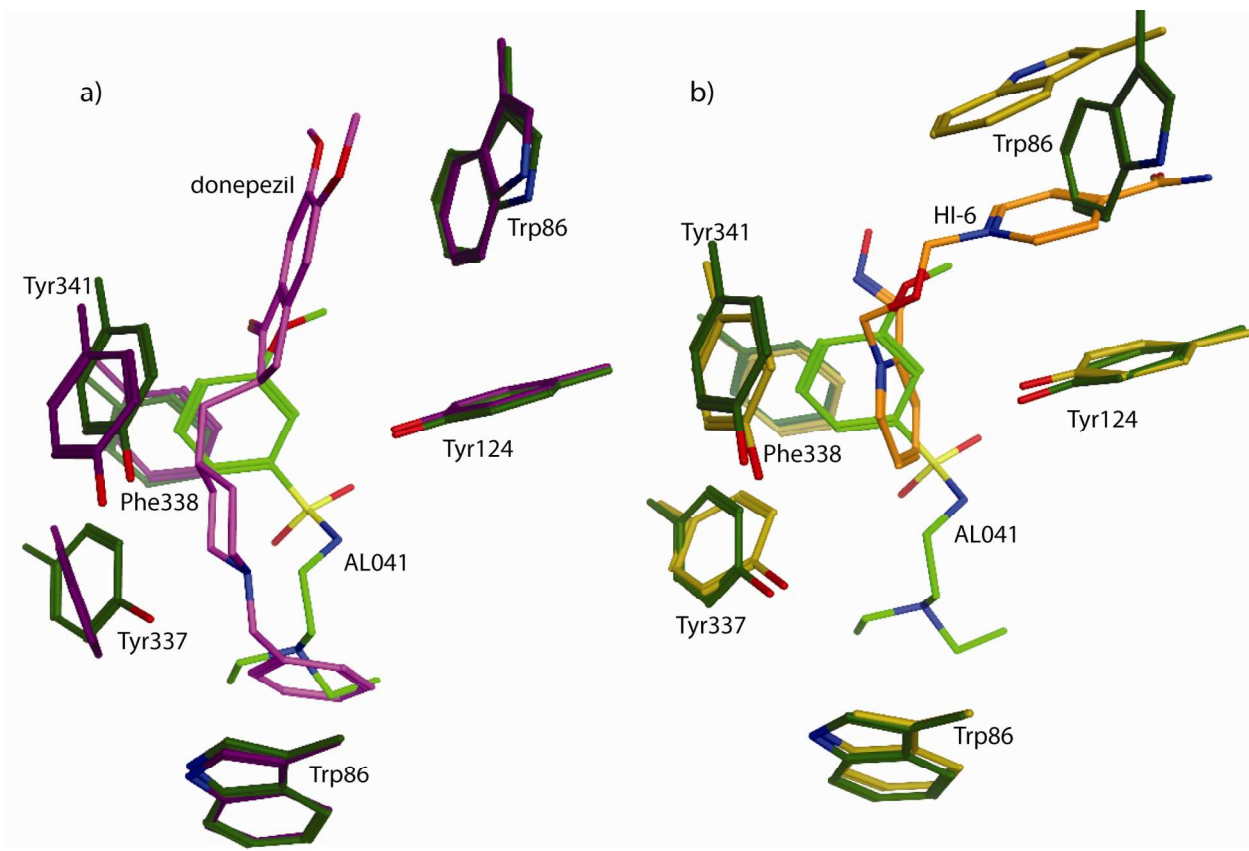


Figure S14. AChE•11 (AL041) (green, *m*AChE numbering) superposed (C_α-carbons) with the MOE software³ on a) AChE•donepezil (purple) crystal structure (PDB code 1EVE,⁴ *Torpedo californica* AChE), and b) AChE•HI-6 (yellow/orange, PDB code 2GYU, *m*AChE).

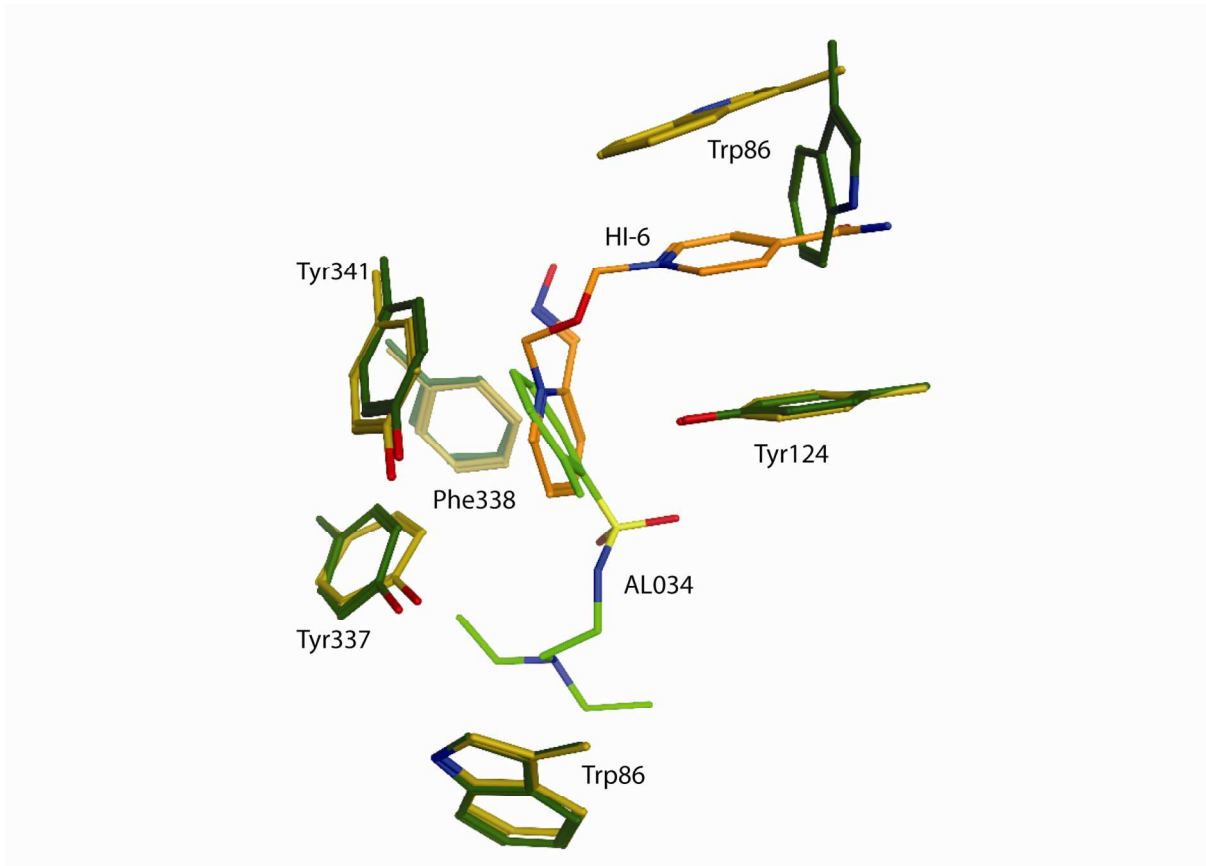
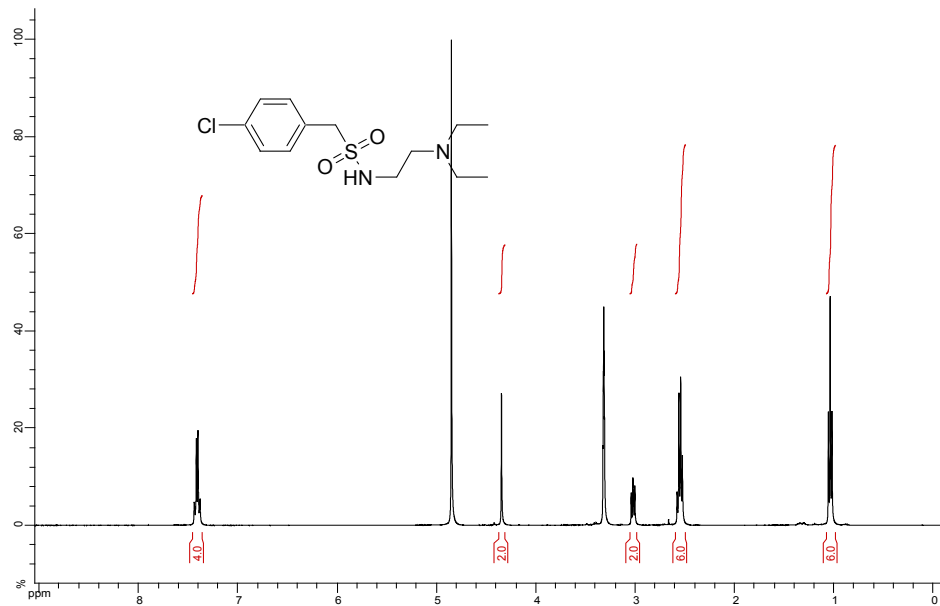


Figure S15. AChE•10 (AL034) (green, *m*AChE numbering) superposed (C_α-carbons) with the MOE software³ on AChE•HI-6 (yellow/orange, PDB code 2GYU, *m*AChE).

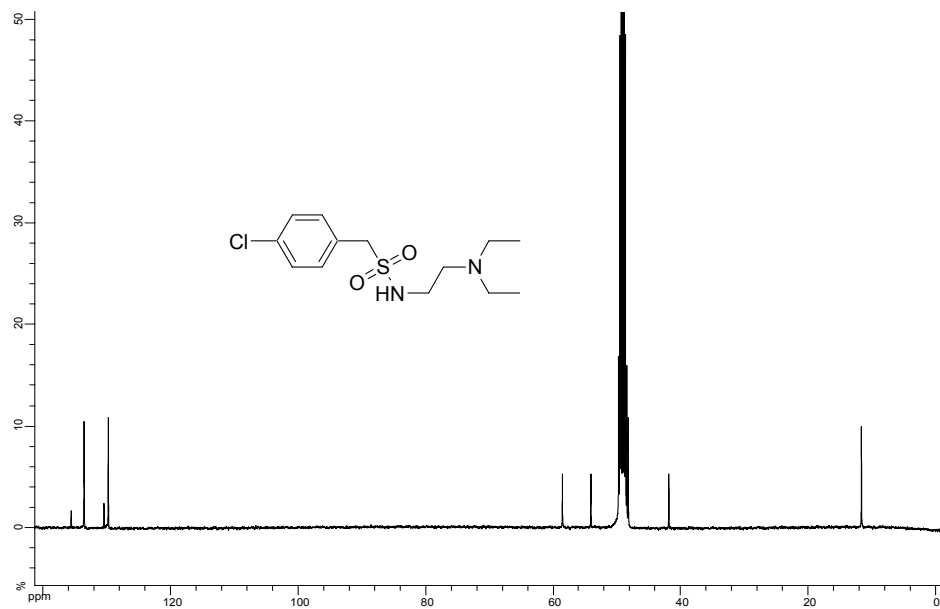
¹H- and ¹³C NMR-spectra

5 (AL011)

¹H NMR

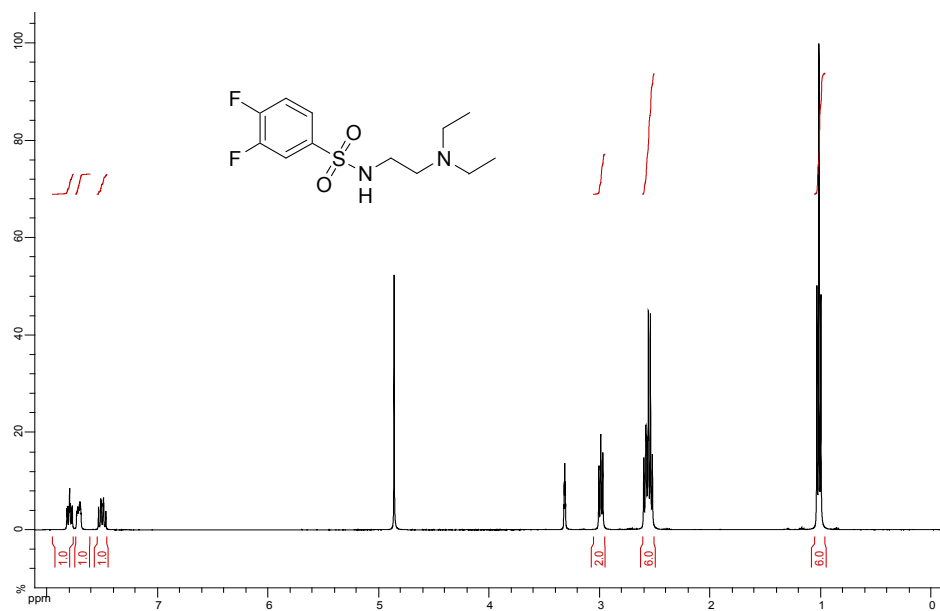


¹³C NMR

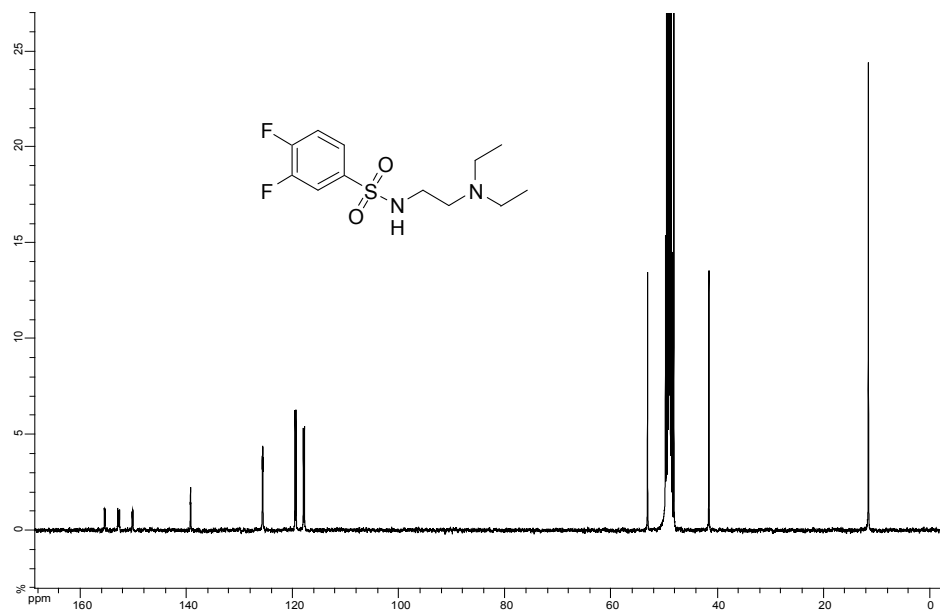


20 (AL023)

¹H NMR

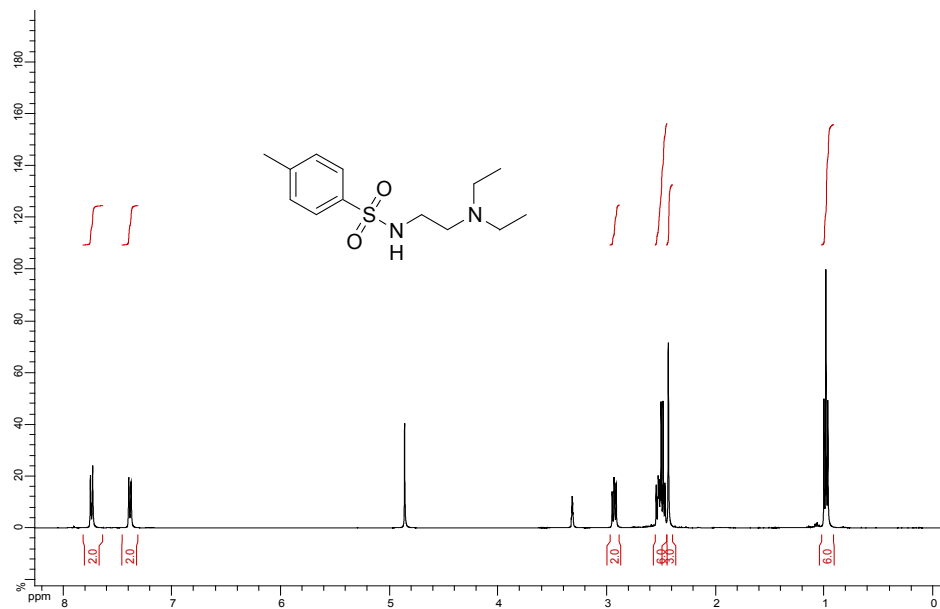


¹³C NMR

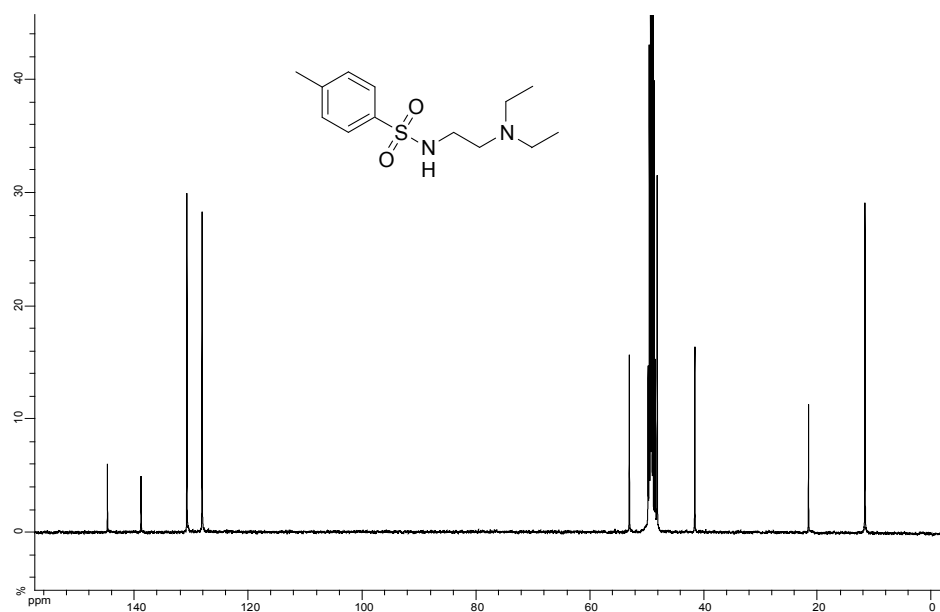


15 (AL025)

¹H NMR

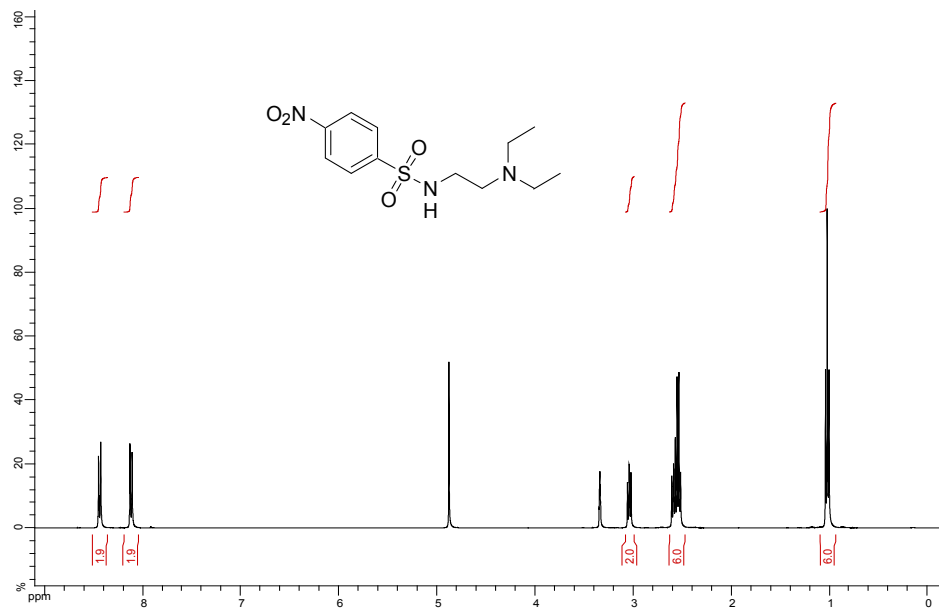


¹³C NMR

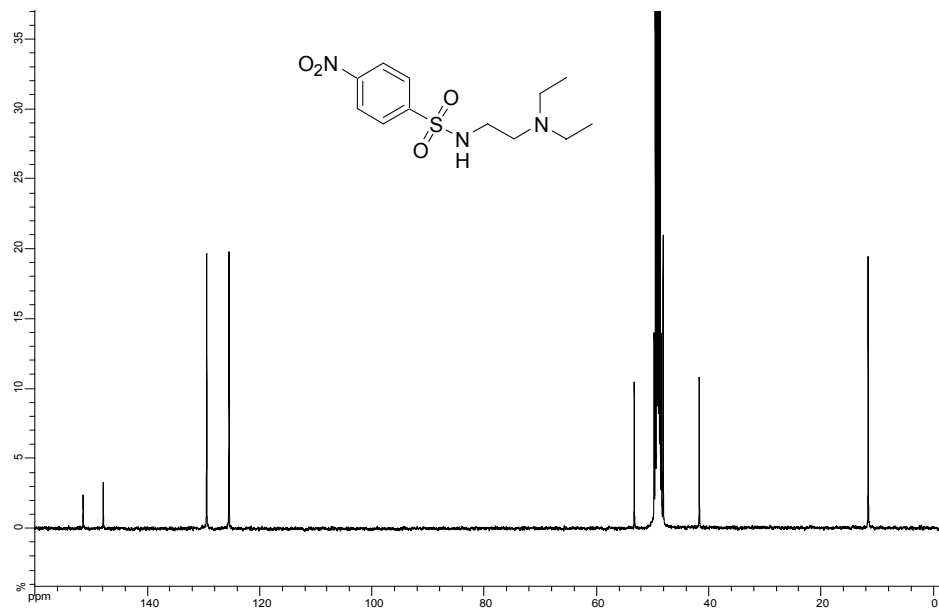


18 (AL026)

¹H NMR

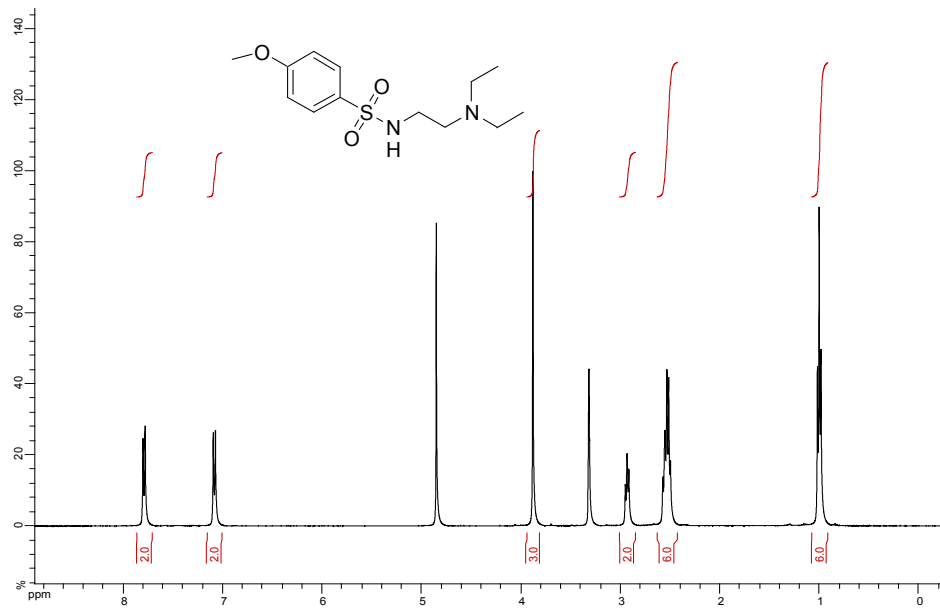


¹³C NMR

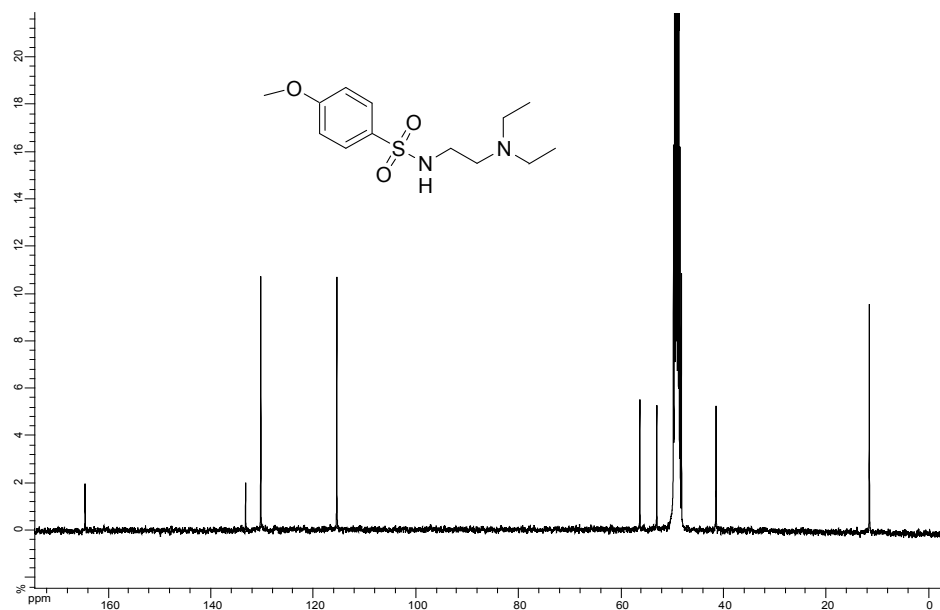


14 (AL027)

^1H NMR

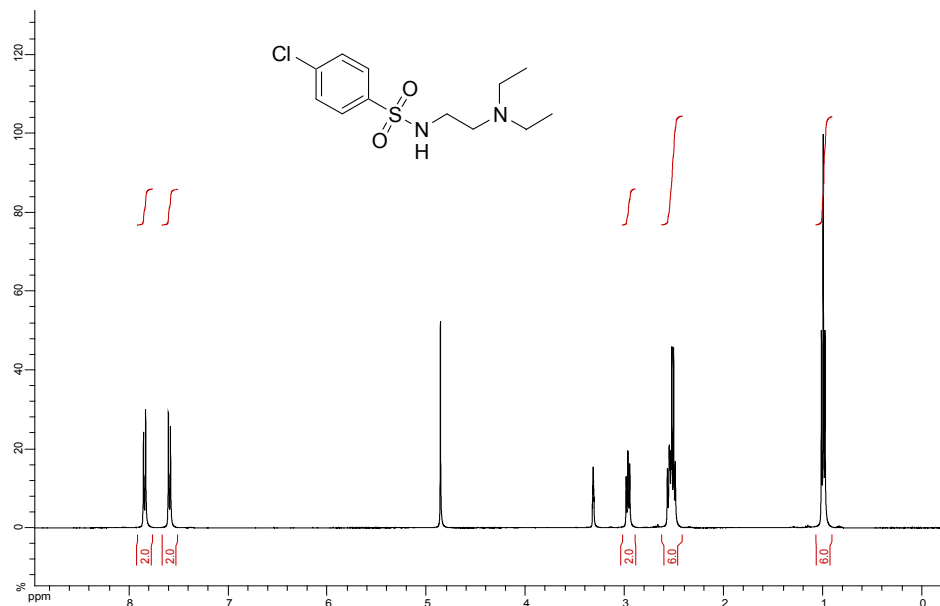


^{13}C NMR

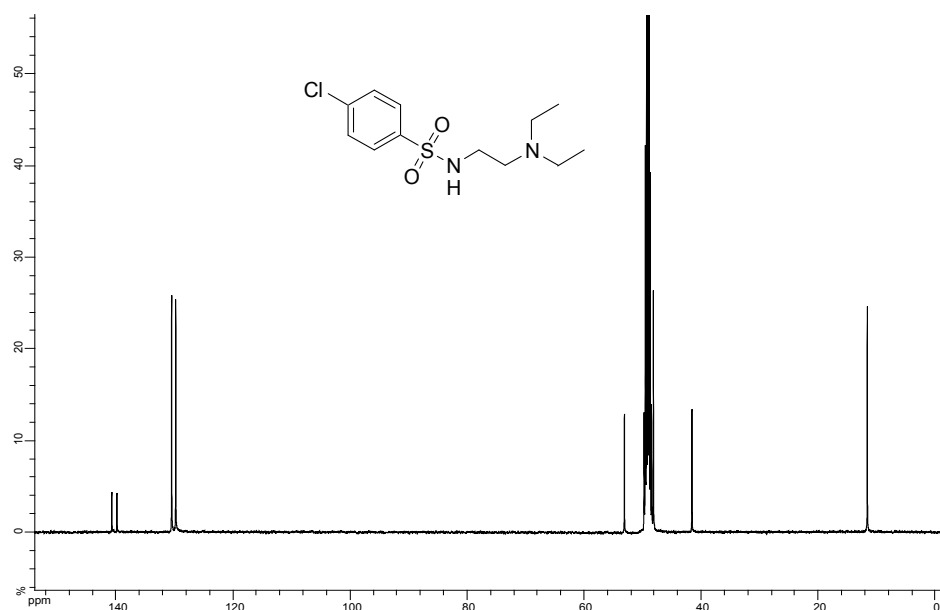


17 (AL028)

¹H NMR

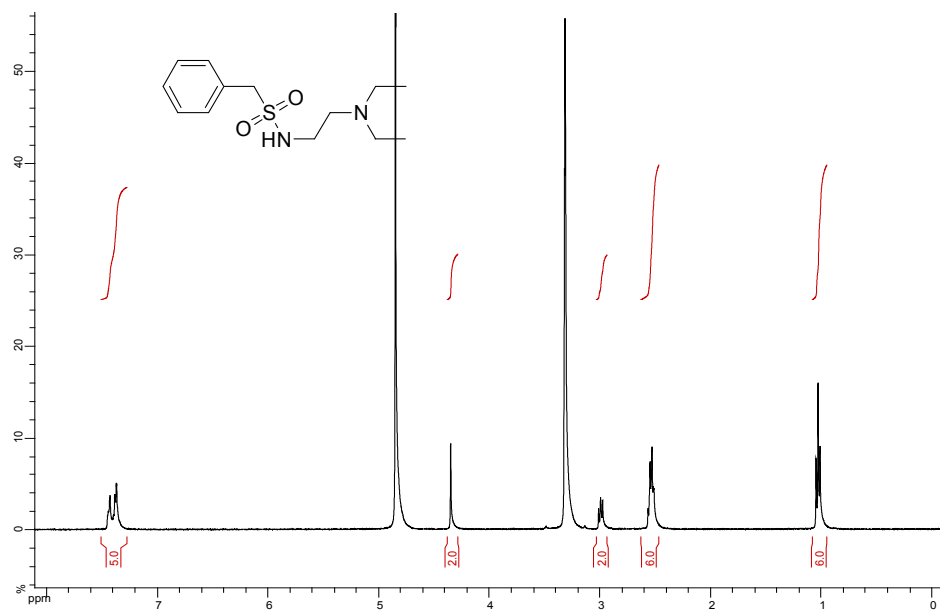


¹³C NMR

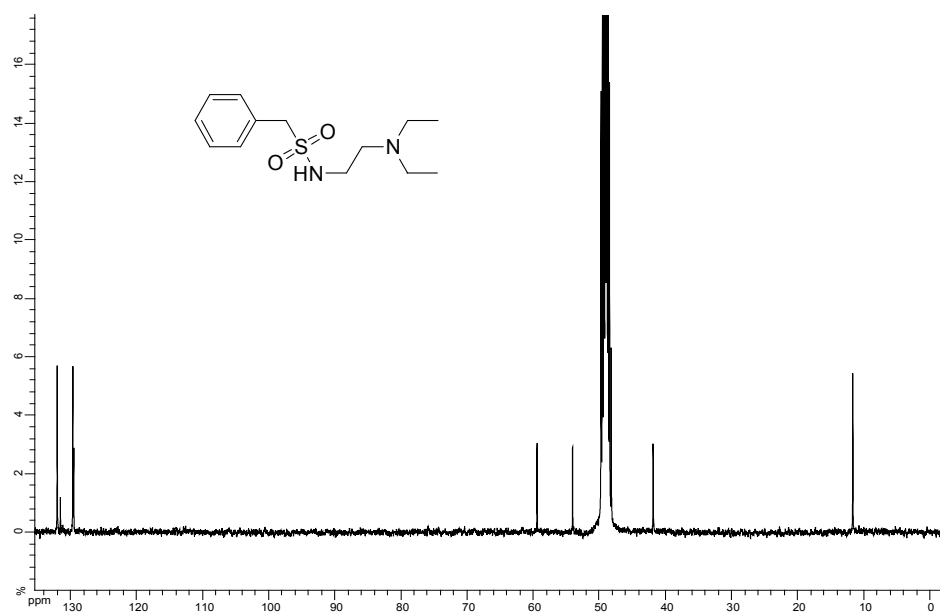


2 (AL029)

¹H NMR

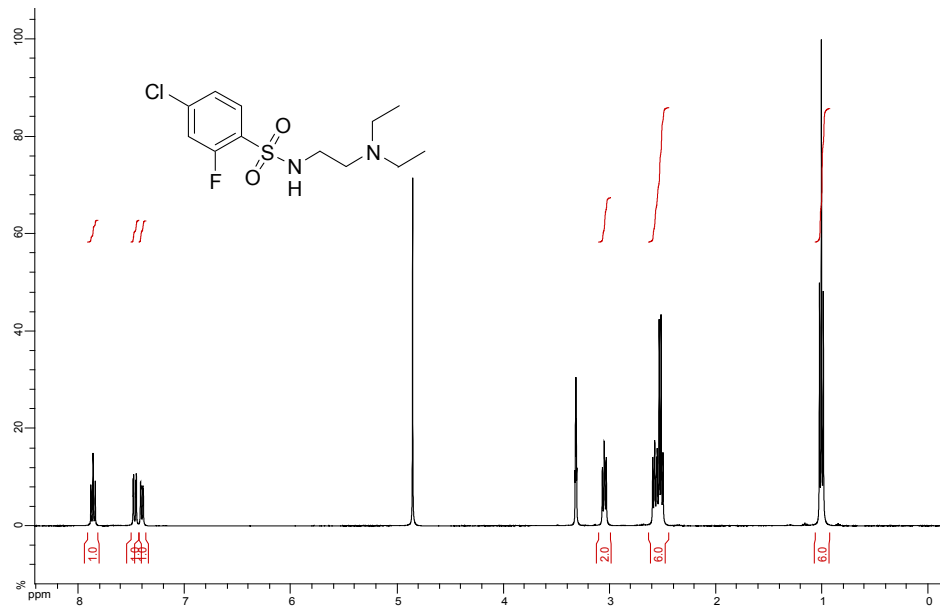


¹³C NMR

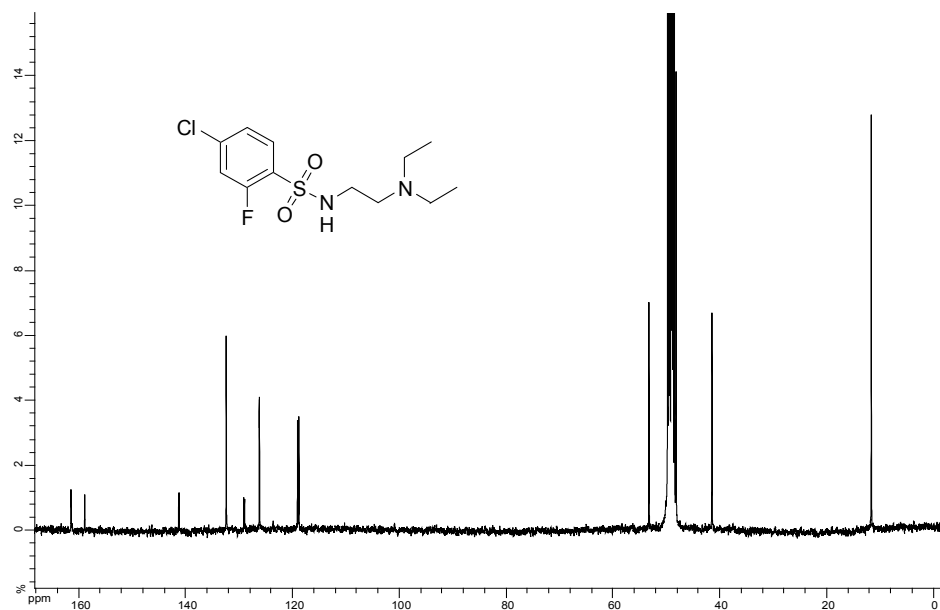


19 (AL030)

¹H NMR

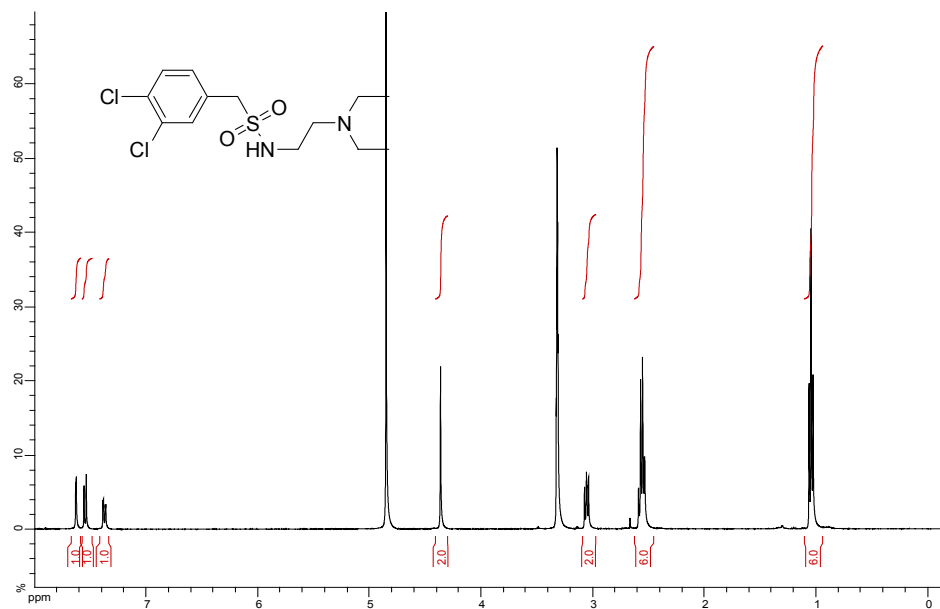


¹³C NMR

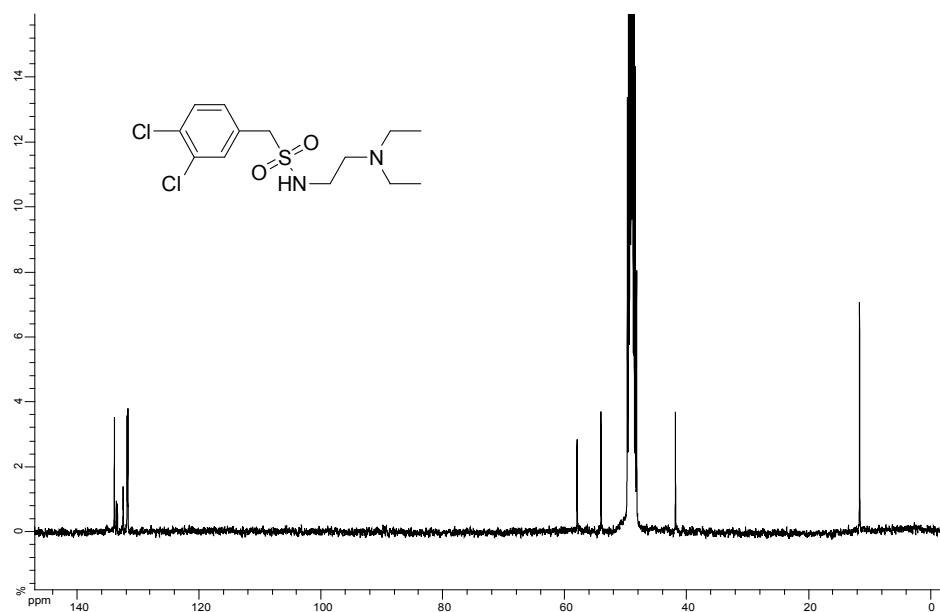


8 (AL031)

^1H NMR

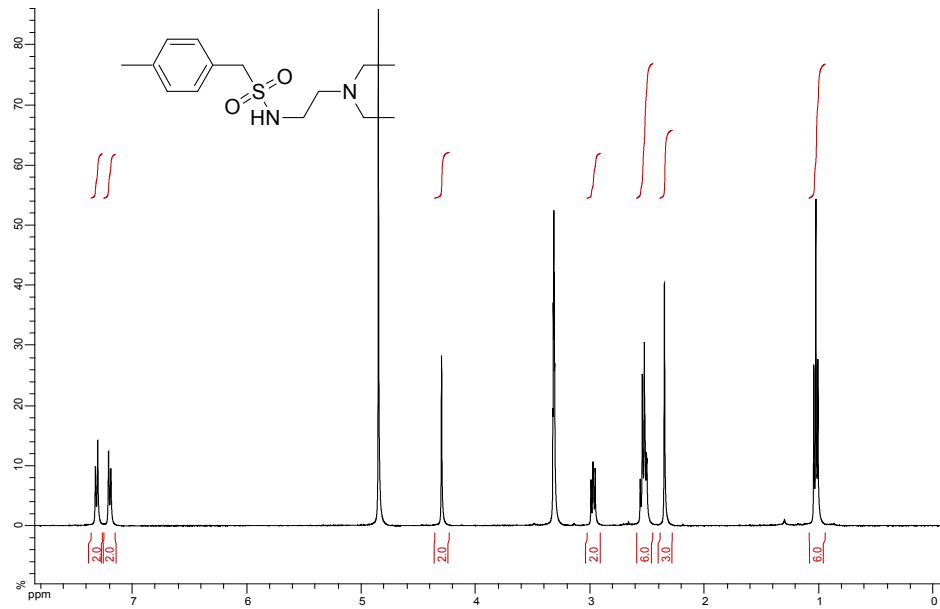


^{13}C NMR

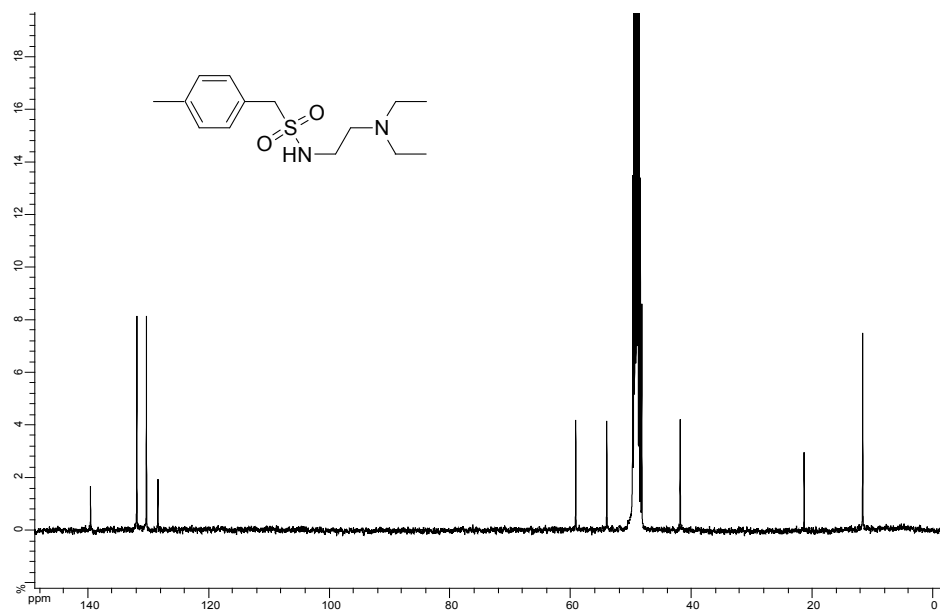


3 (AL032)

¹H NMR

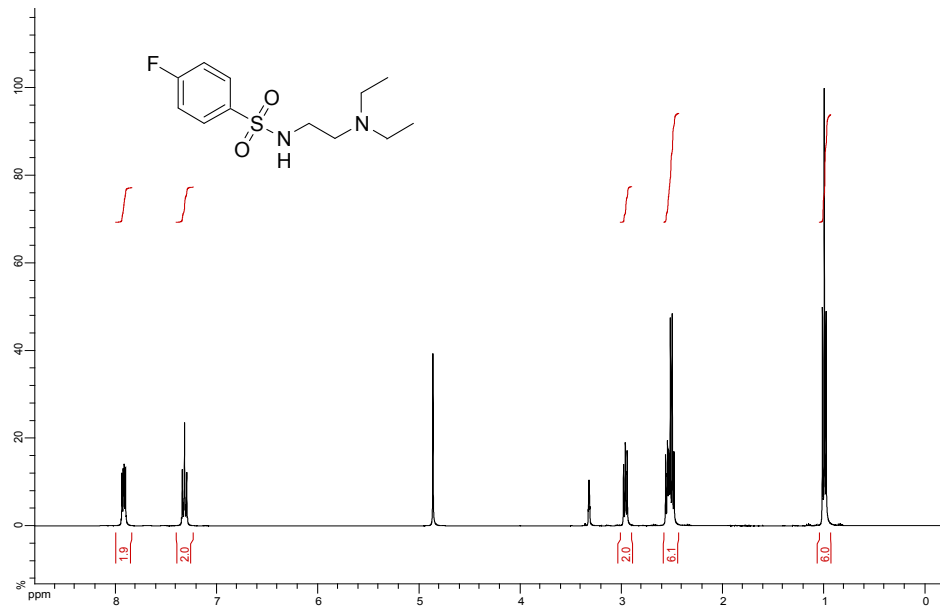


¹³C NMR

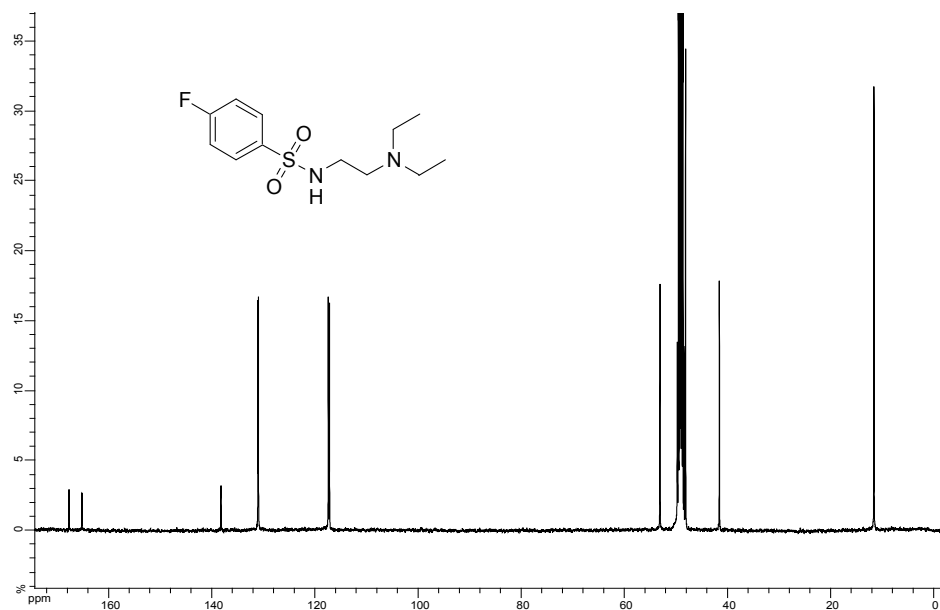


16 (AL033)

¹H NMR

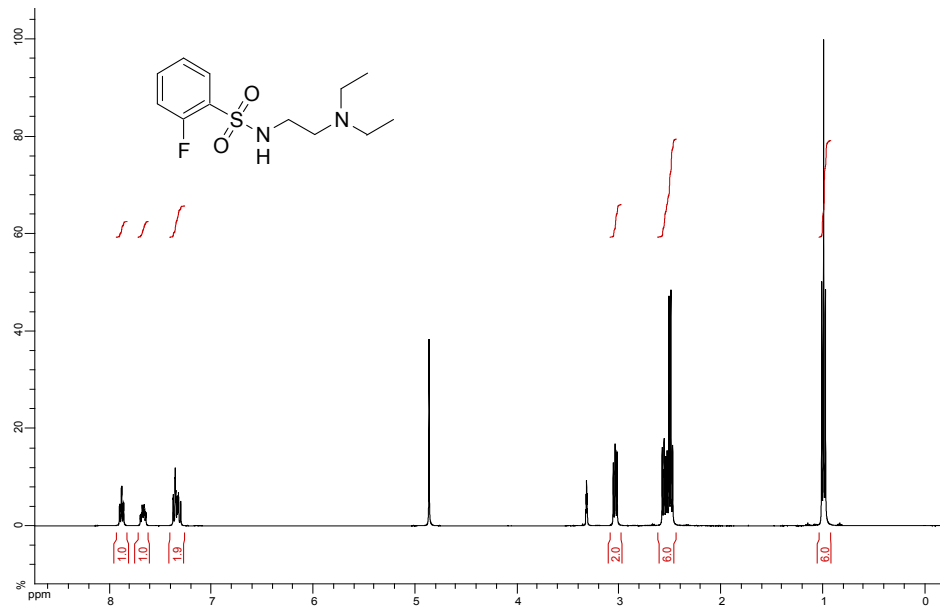


¹³C NMR

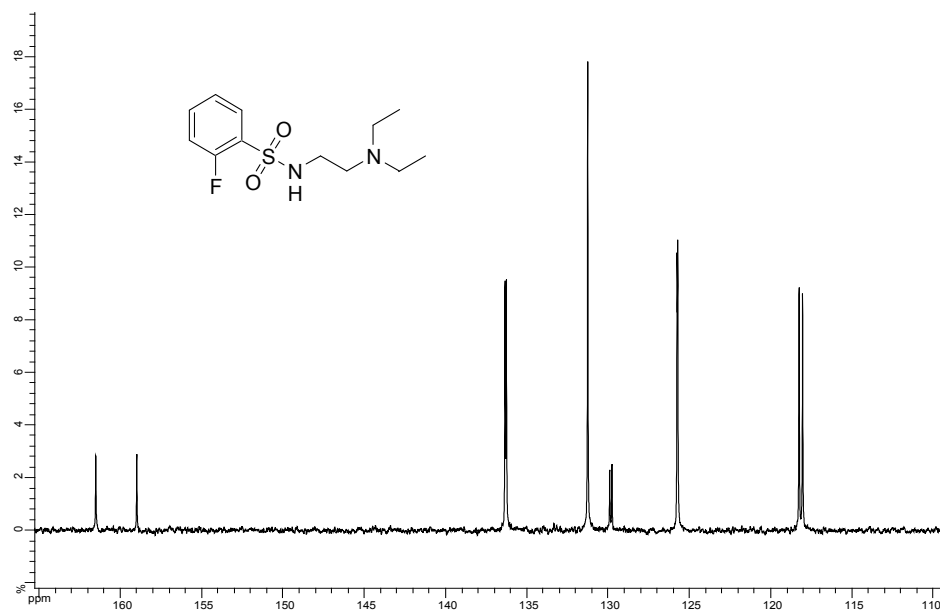


10 (AL034)

¹H NMR

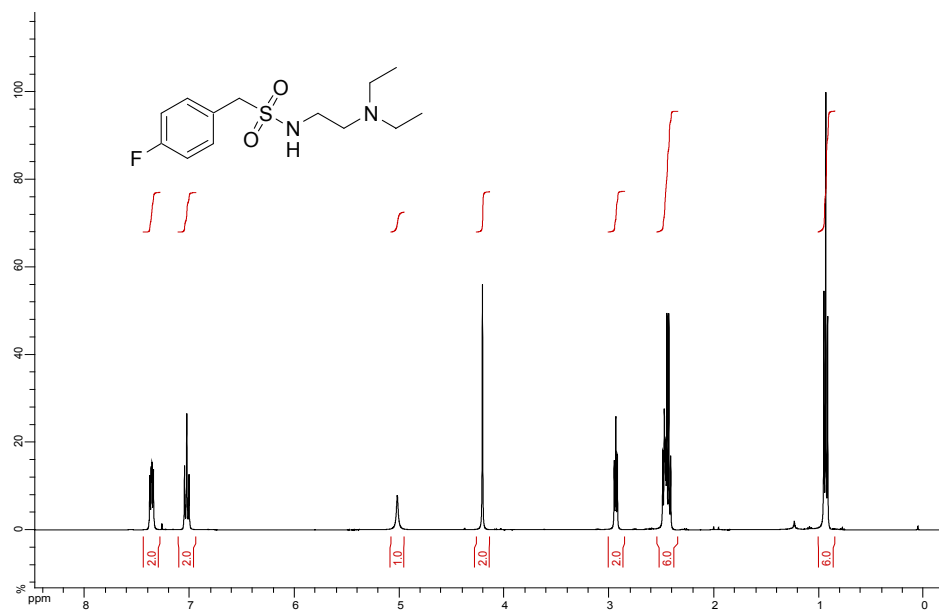


¹³C NMR

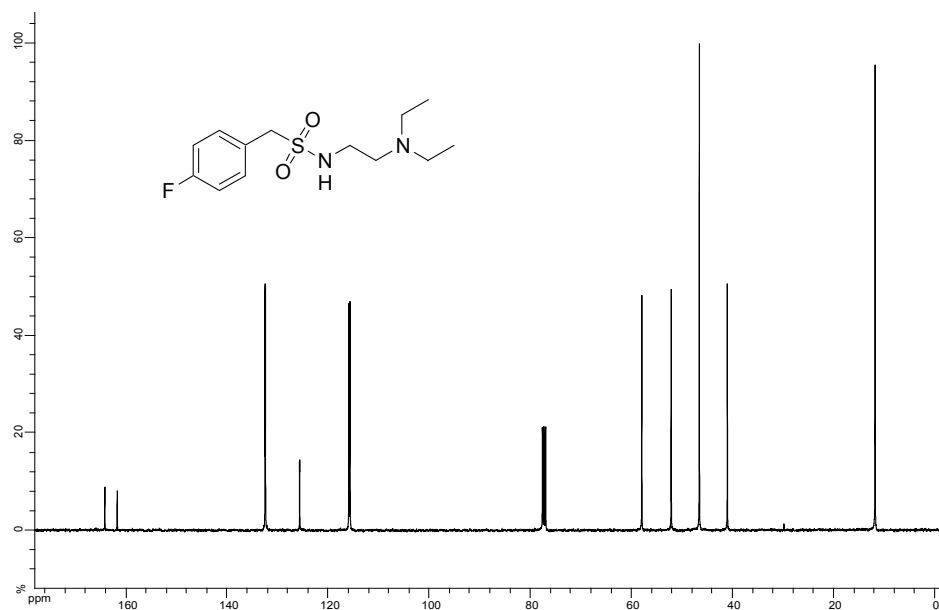


4 (AL036)

¹H NMR

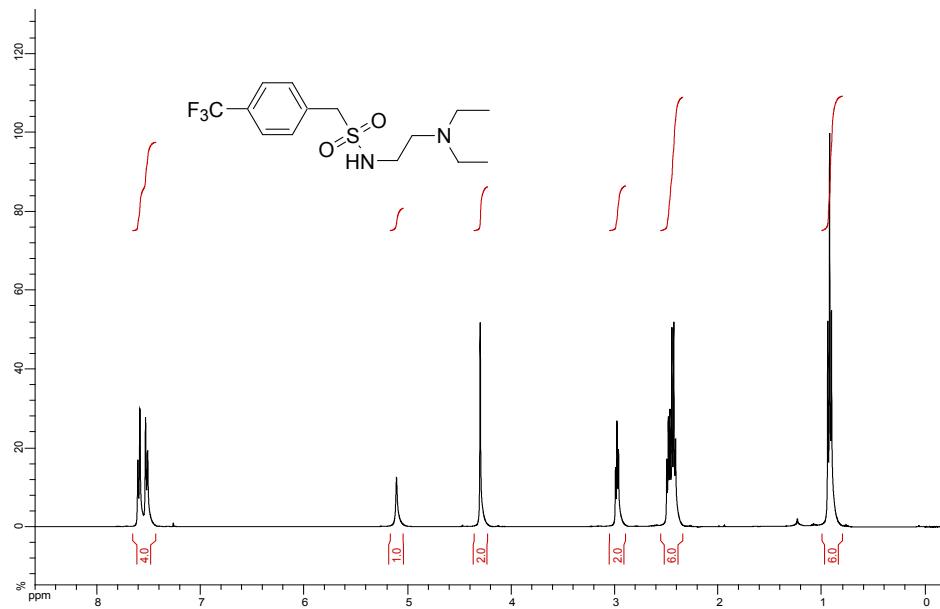


¹³C NMR

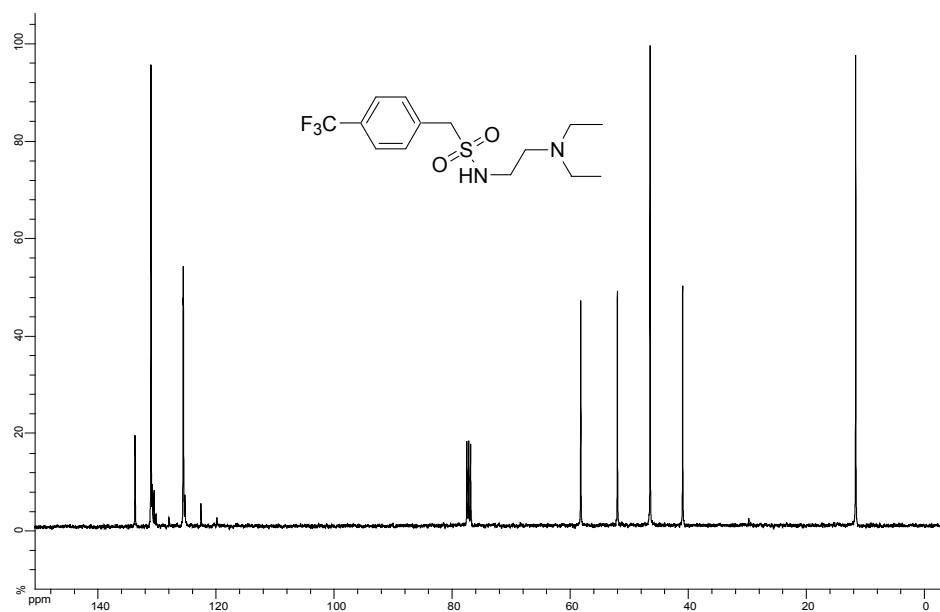


6 (AL037)

¹H NMR

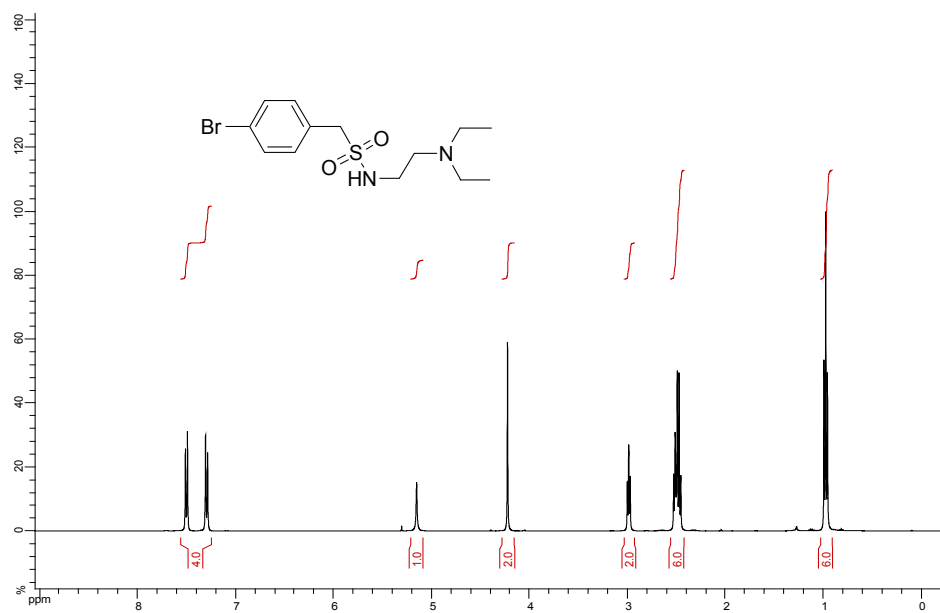


¹³C NMR

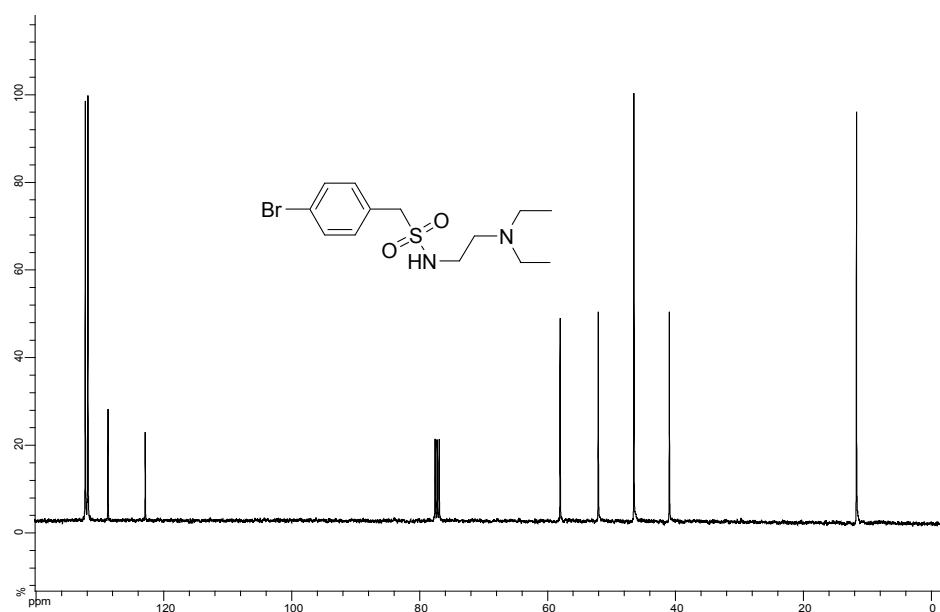


7 (AL038)

¹H NMR

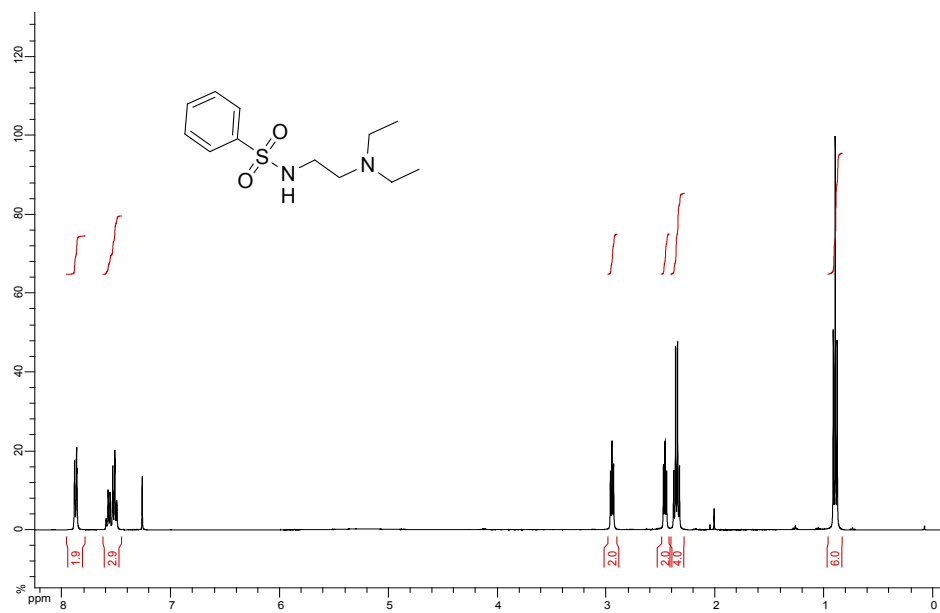


¹³C NMR

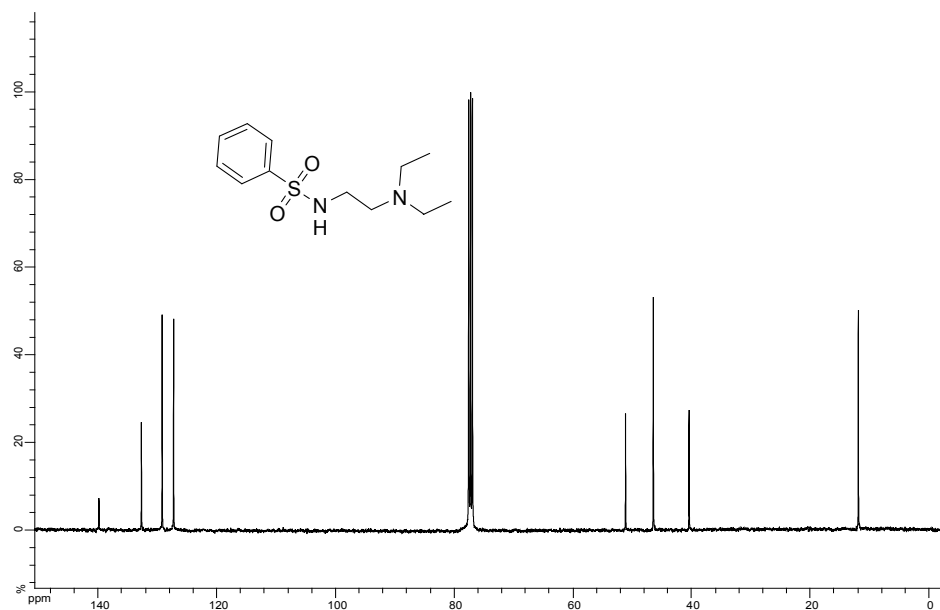


9 (AL039)

¹H NMR

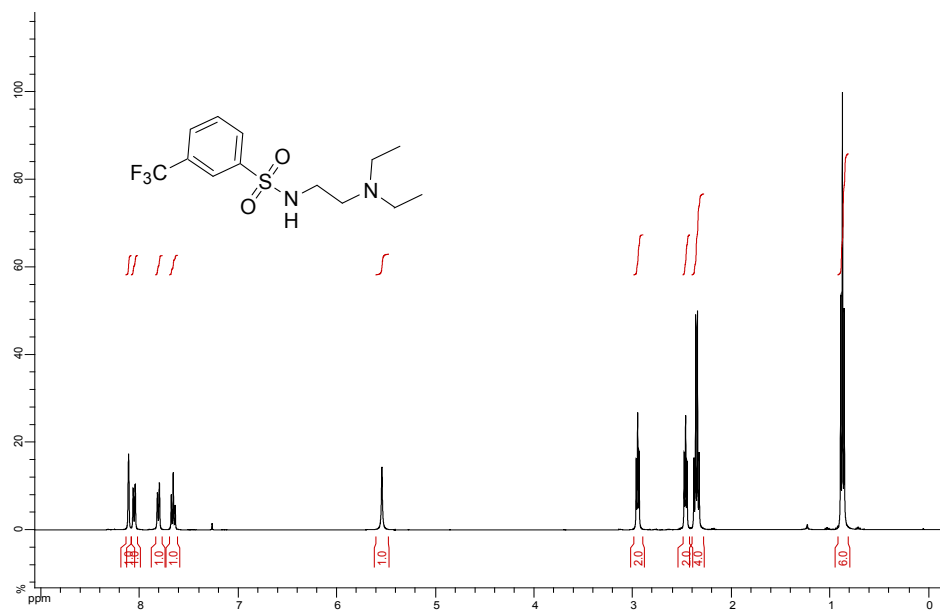


¹³C NMR

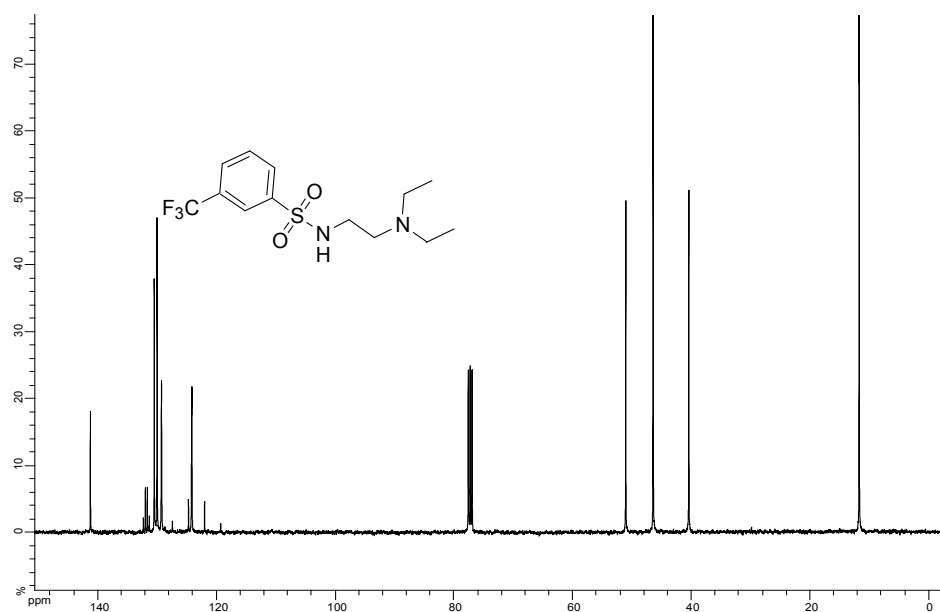


12 (AL040)

¹H NMR

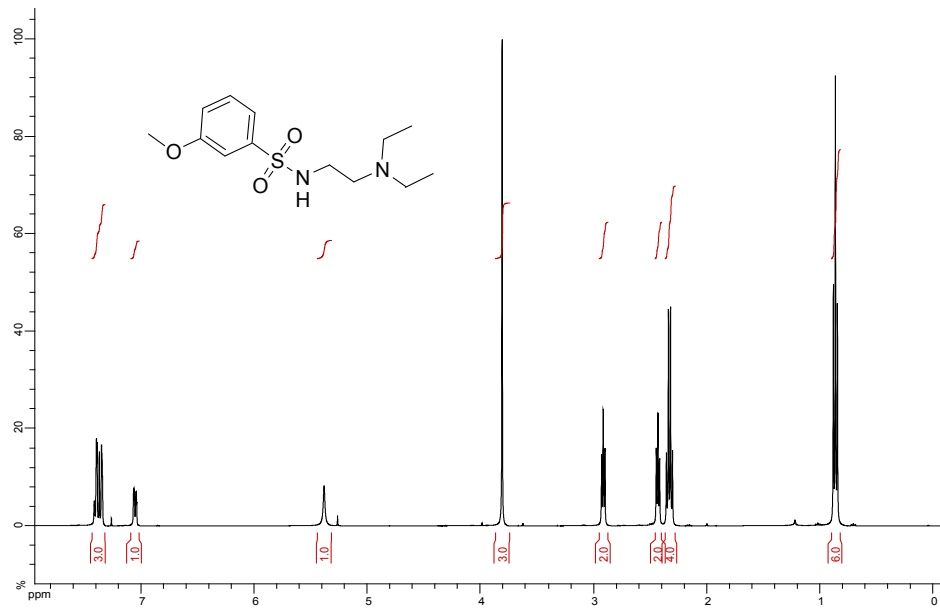


¹³C NMR

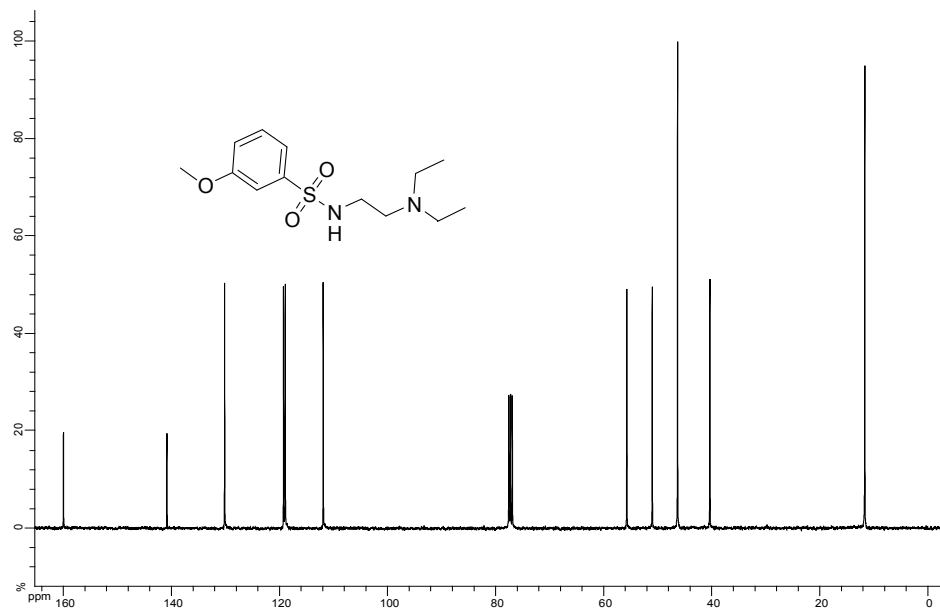


11 (AL041)

¹H NMR

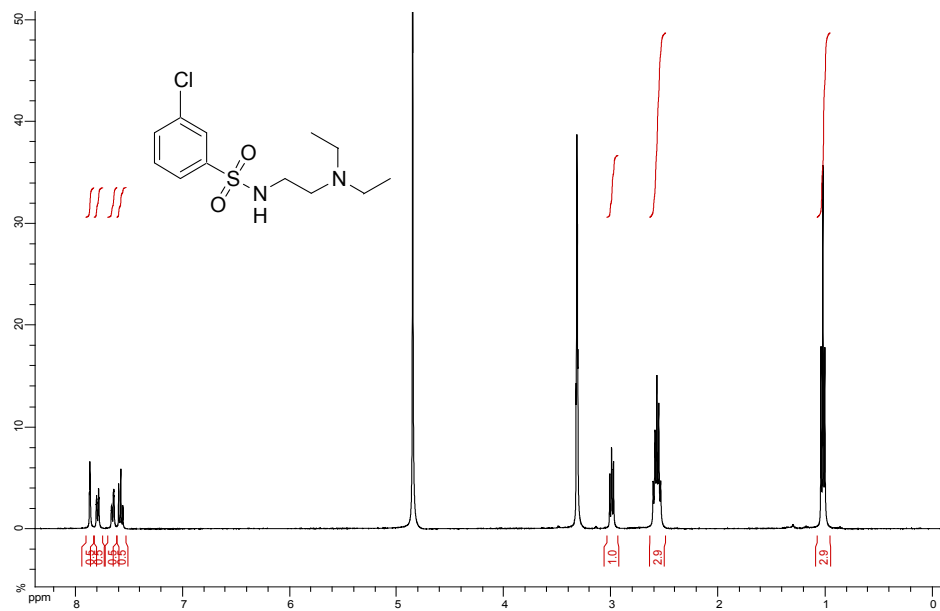


¹³C NMR

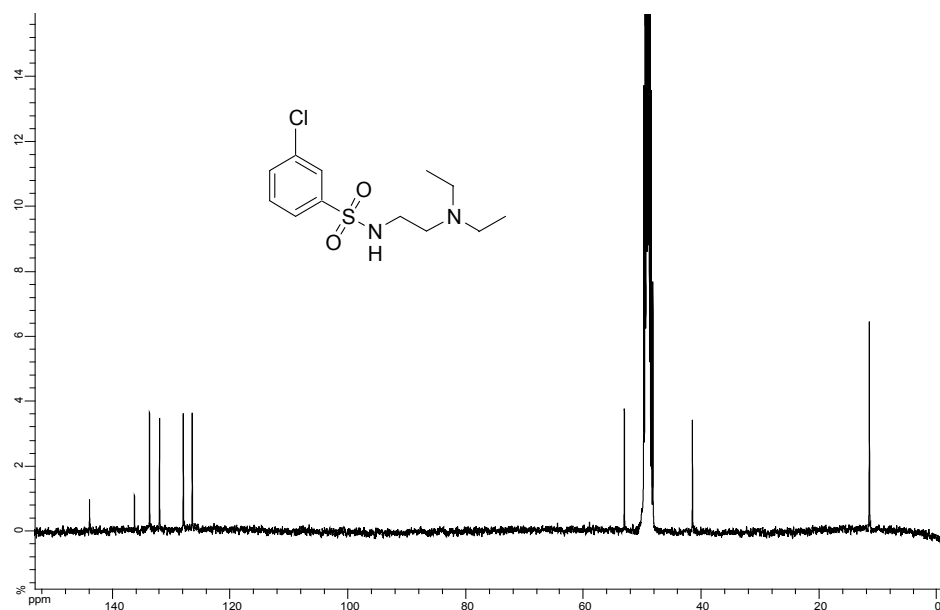


13 (AL024)

^1H NMR

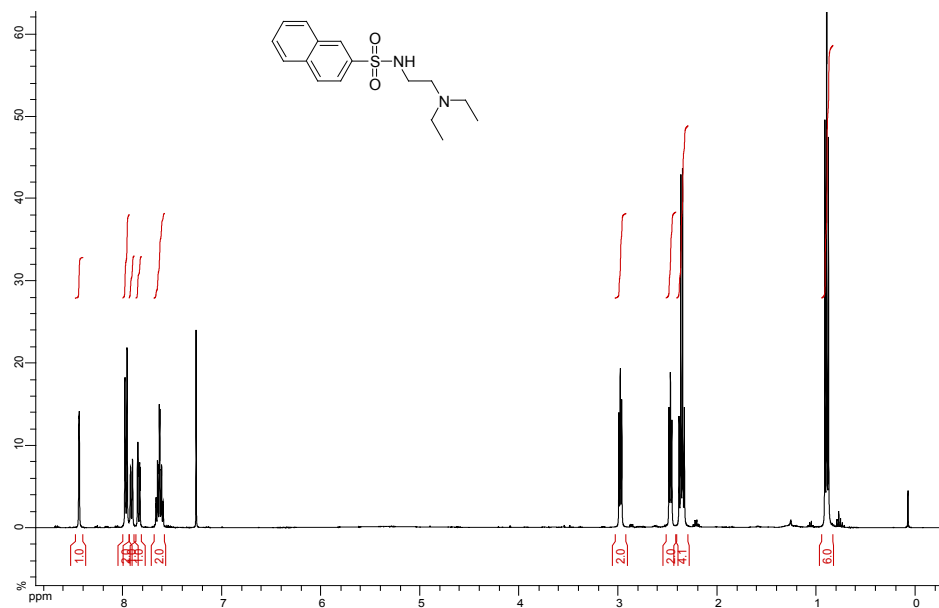


^{13}C NMR

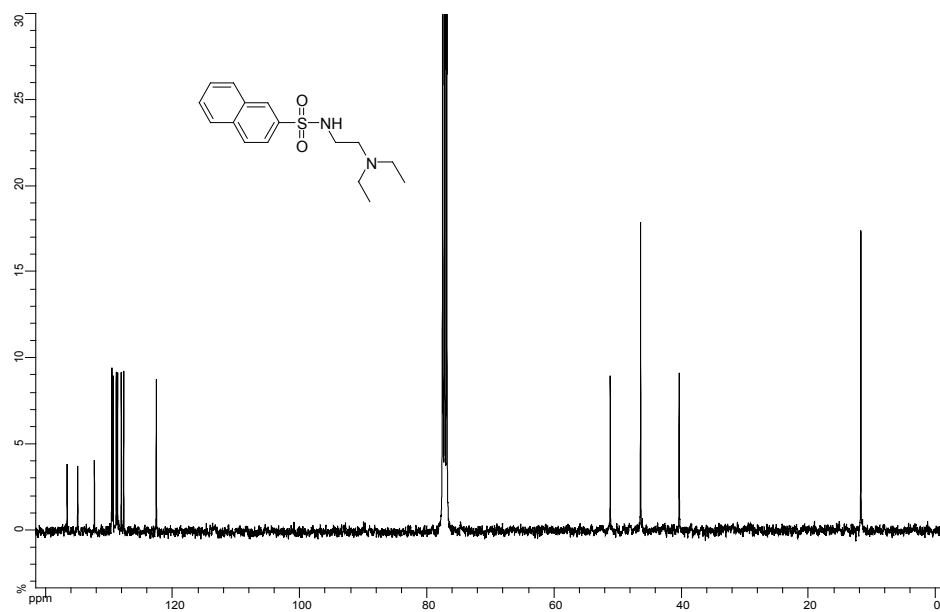


22 (AL143)

¹H NMR

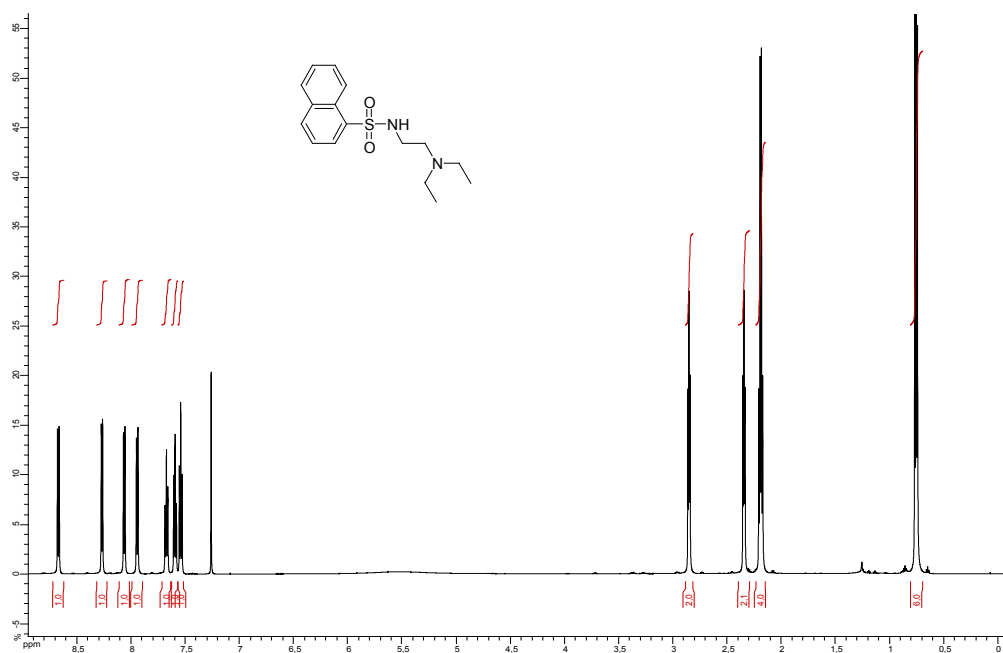


¹³C NMR

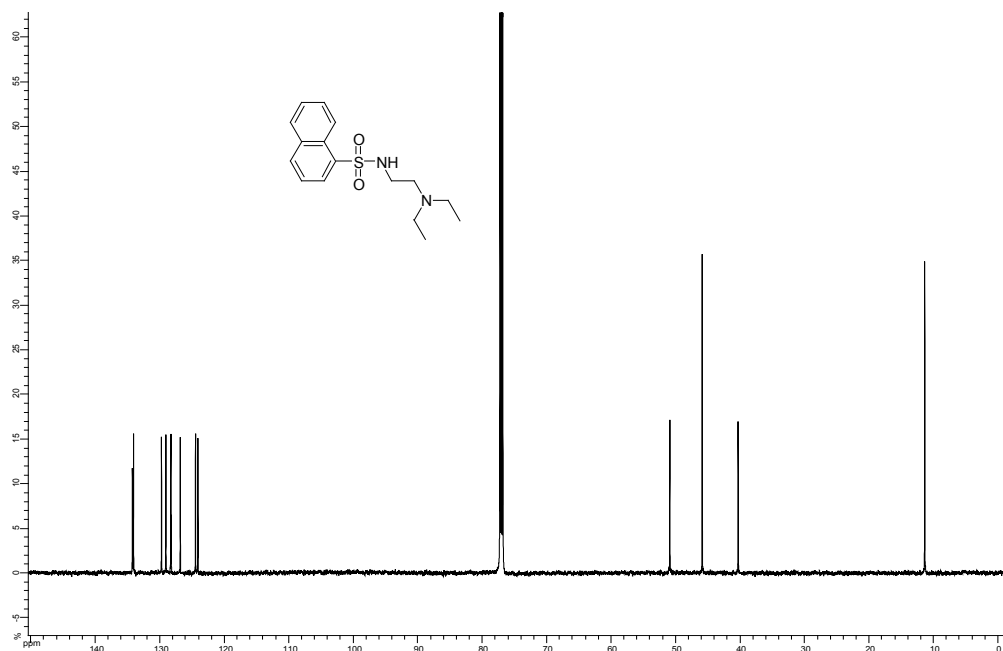


21 (AL144)

^1H NMR

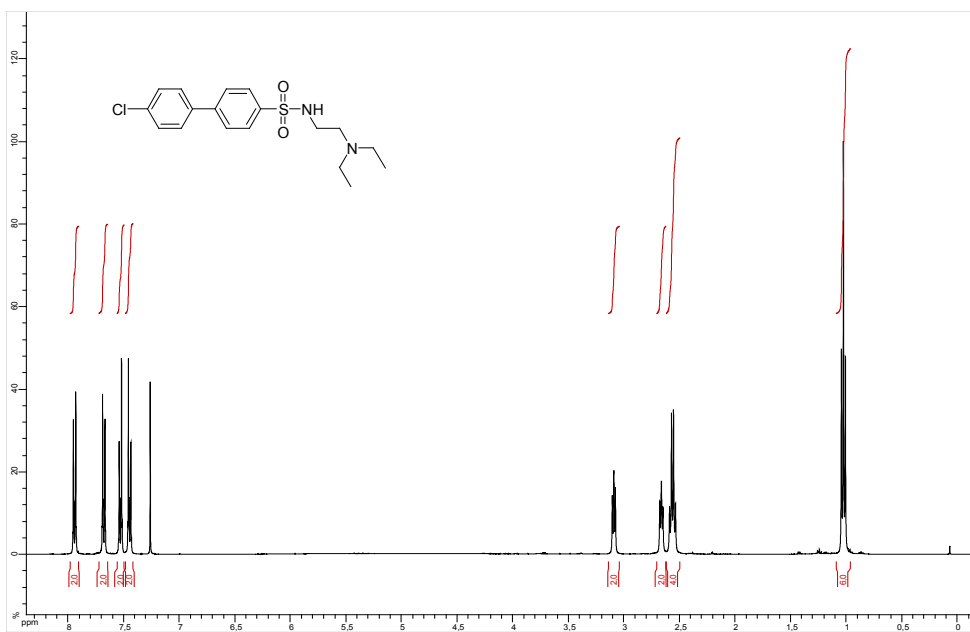


^{13}C NMR

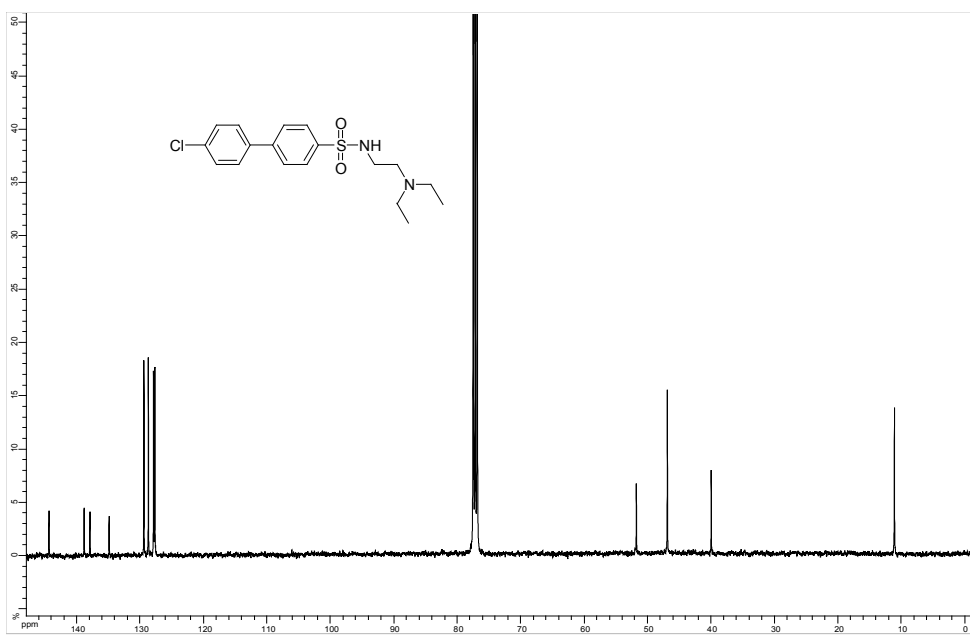


23 (AL149)

¹H NMR

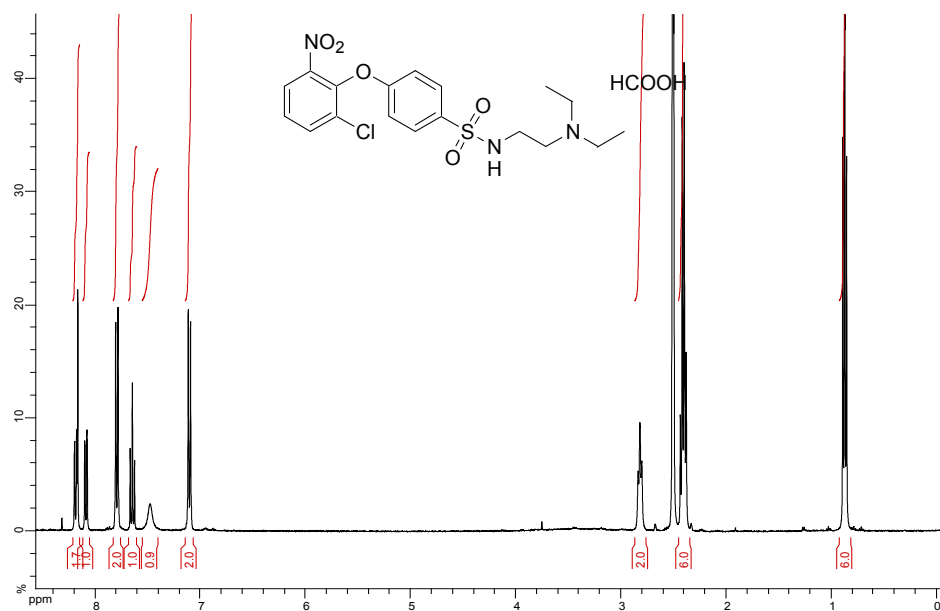


¹³C NMR

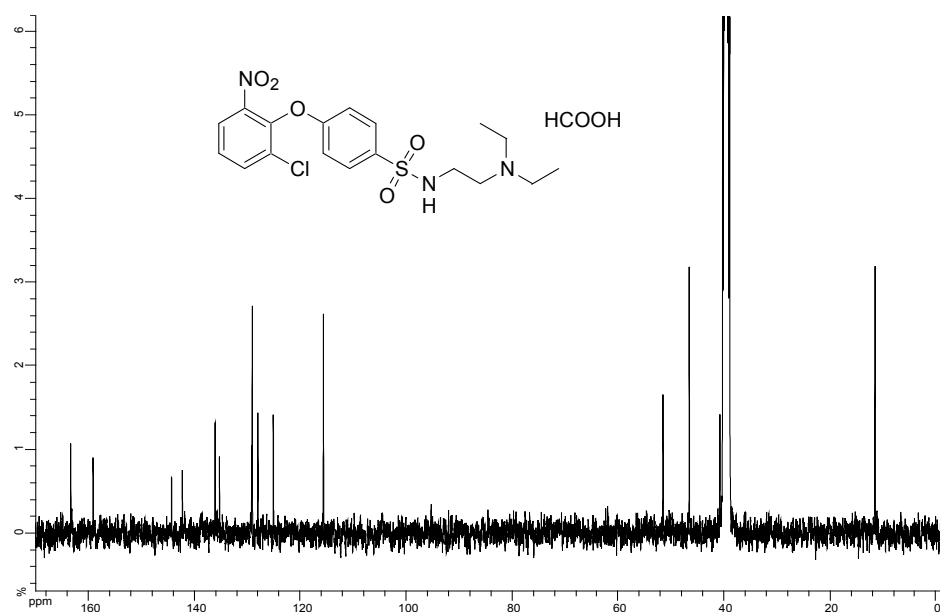


24 (AL151)

¹H NMR

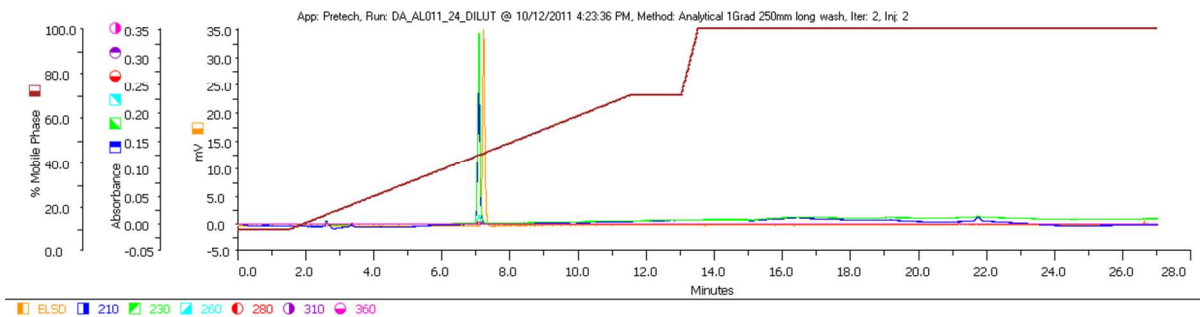


¹³C NMR

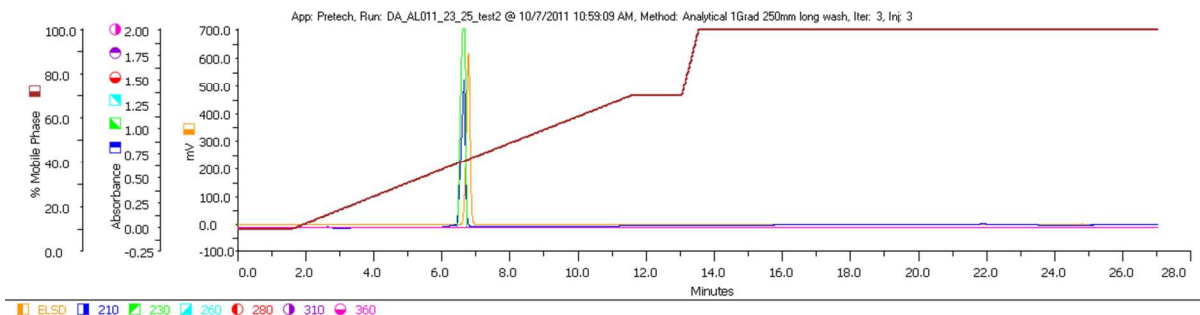


Analytical HPLC spectra

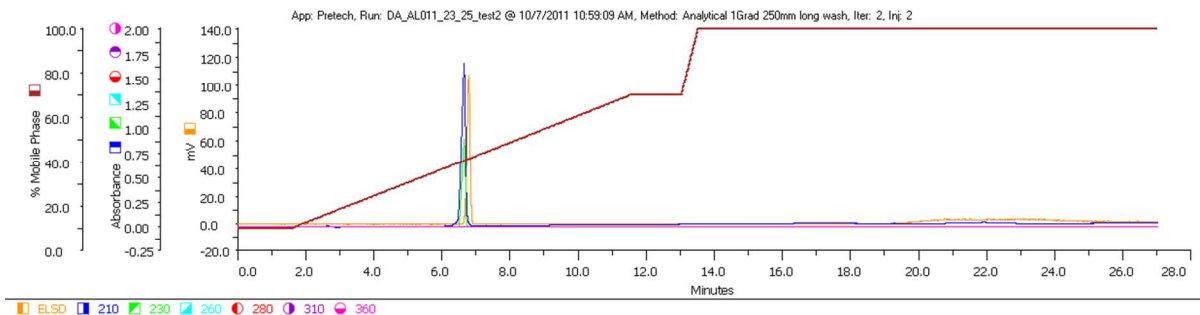
5 (AL011)



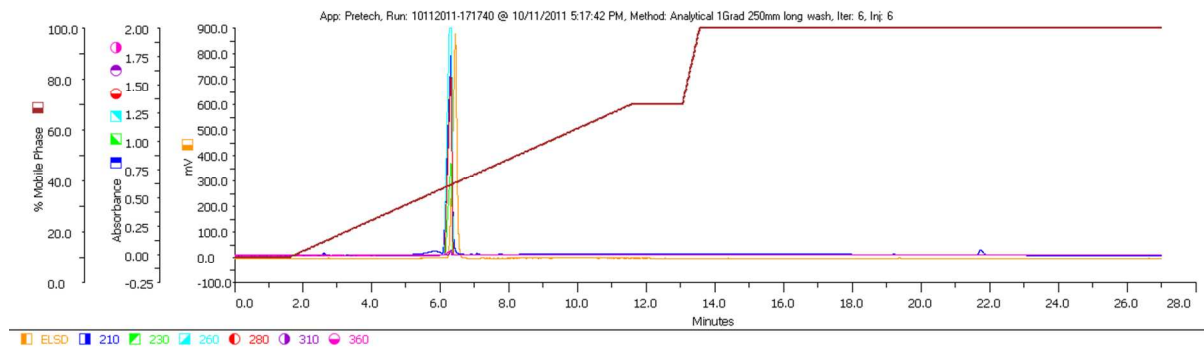
20 (AL023)



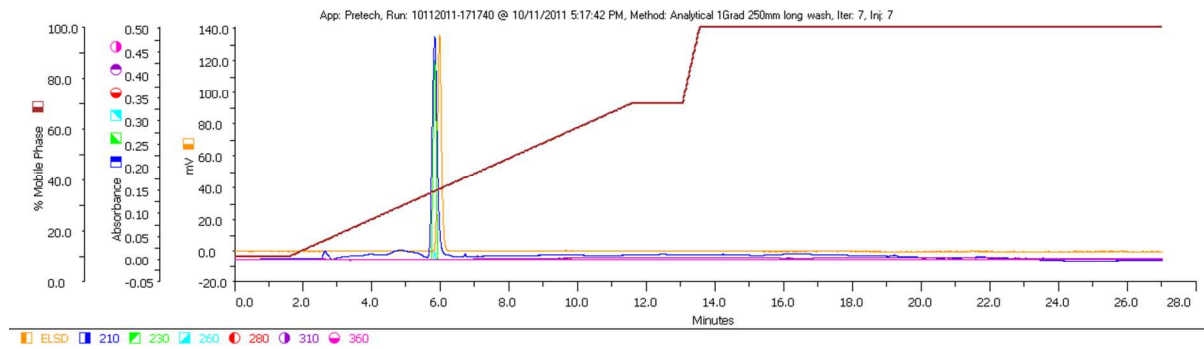
15 (AL025)



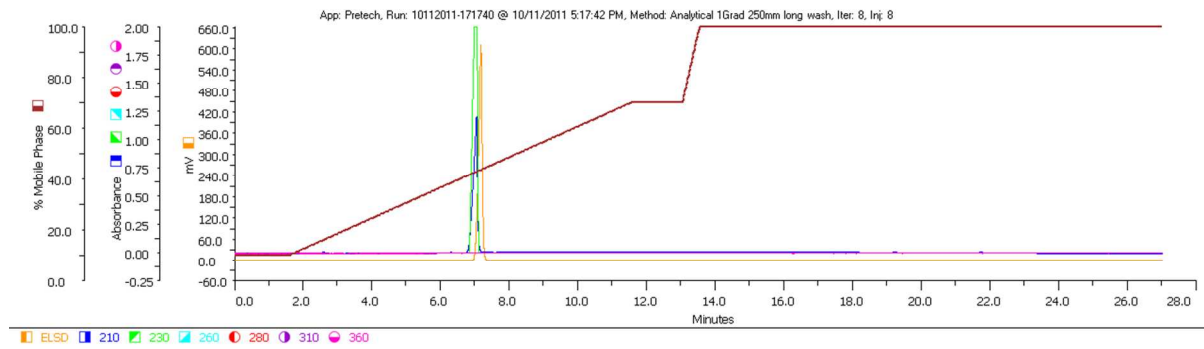
18 (AL026)



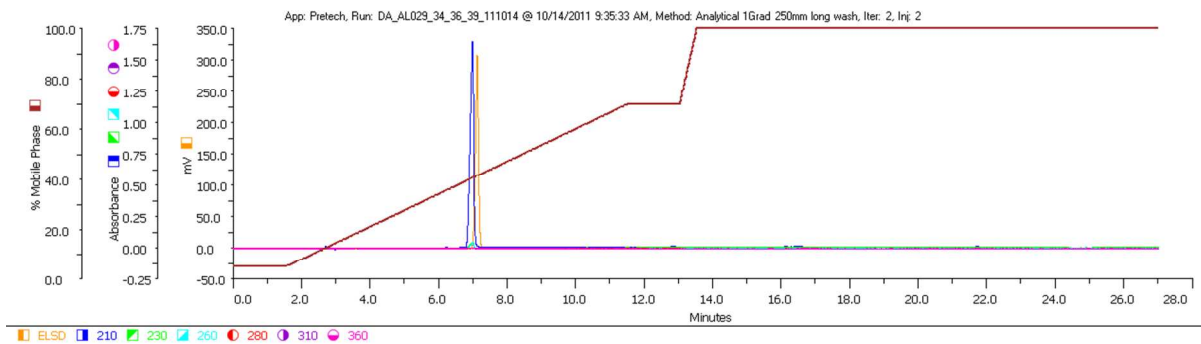
14 (AL027)



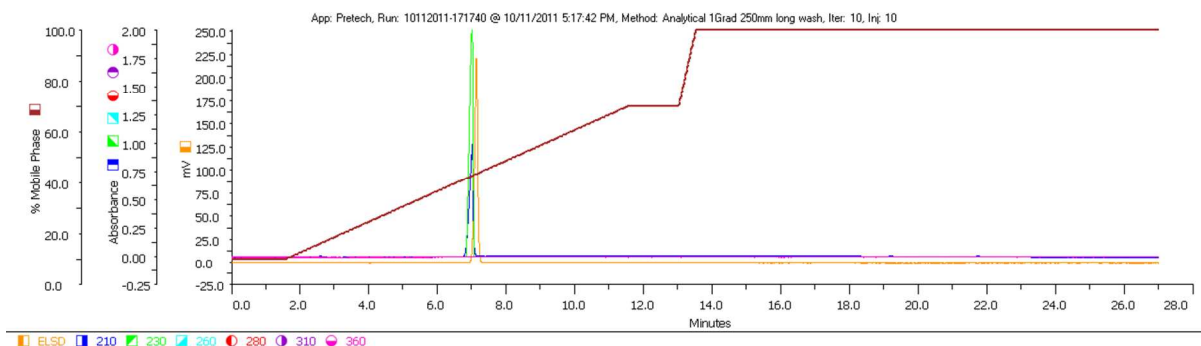
17 (AL028)



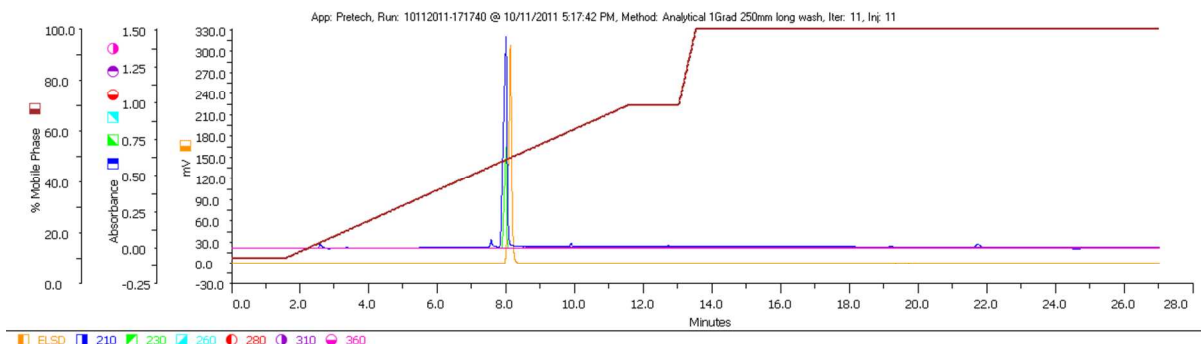
2 (AL029)



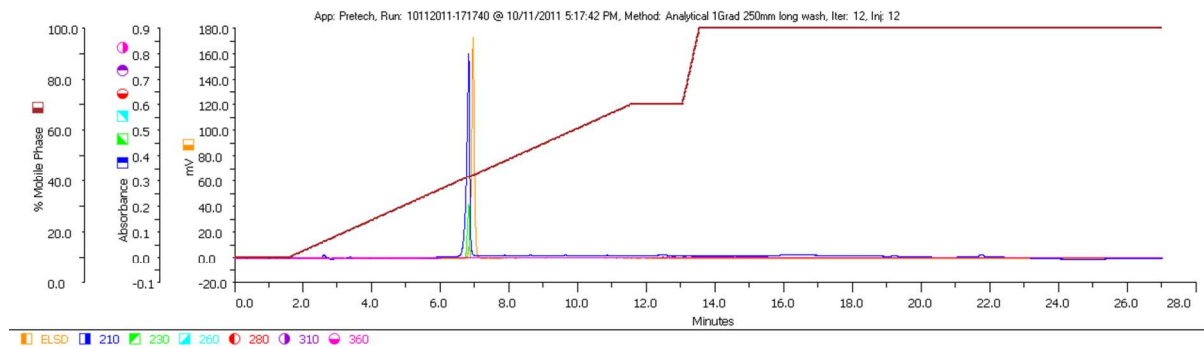
19 (AL030)



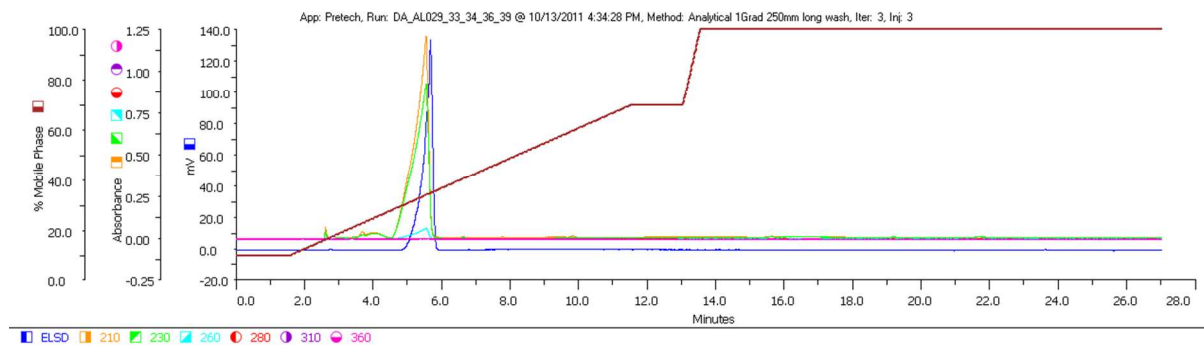
8 (AL031)



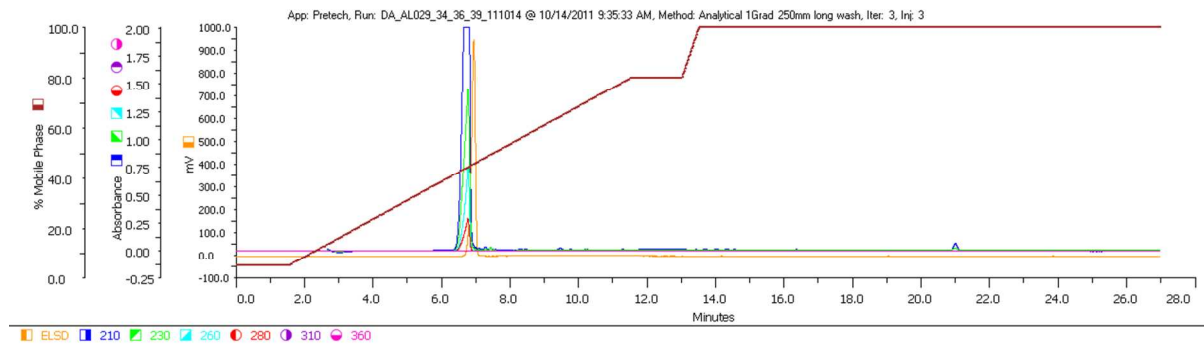
3 (AL032)



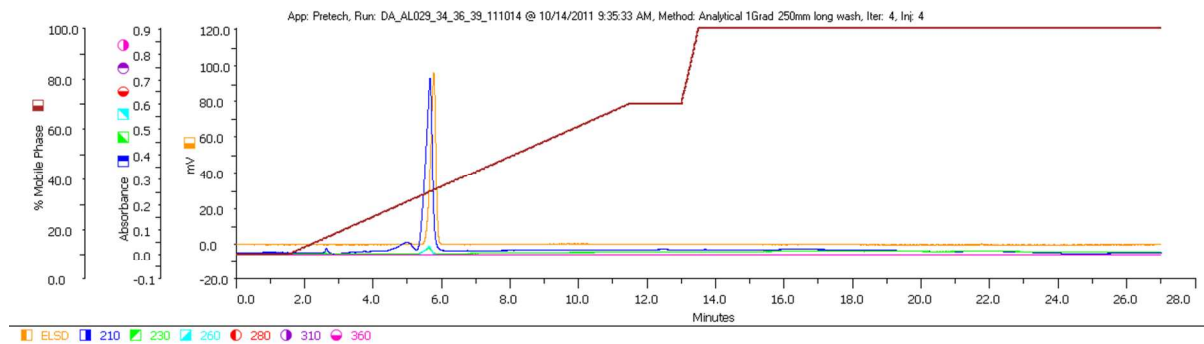
16 (AL033)



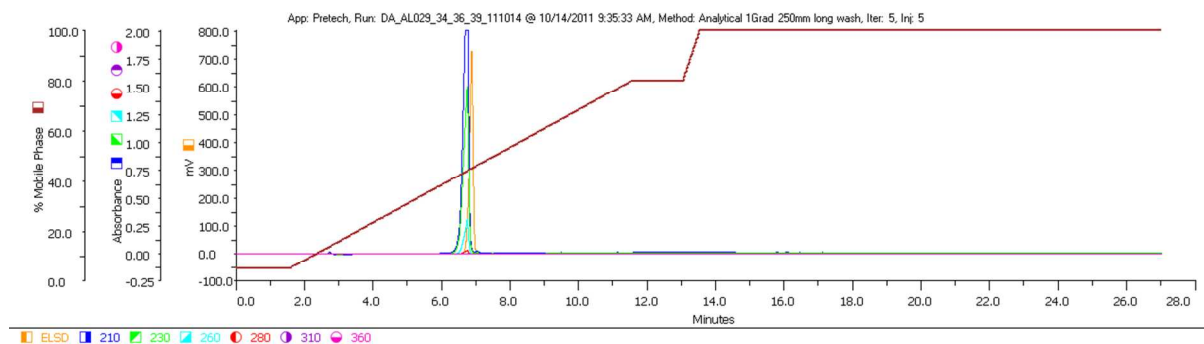
10 (AL034)



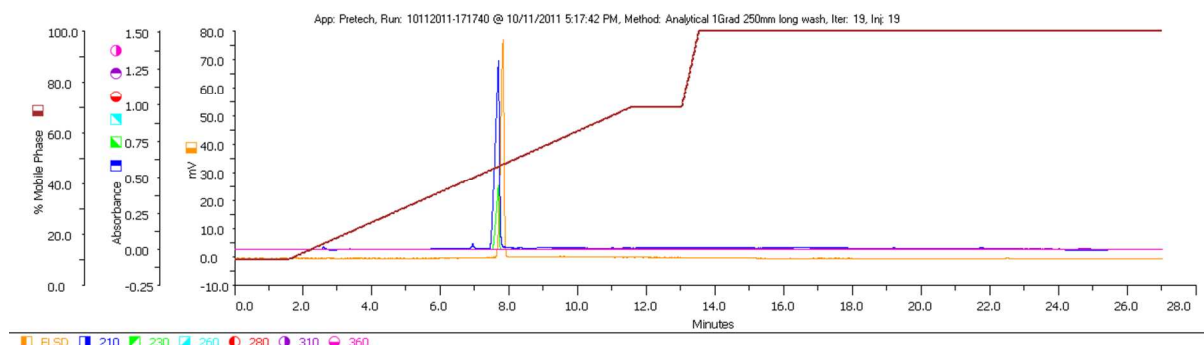
4 (AL036)



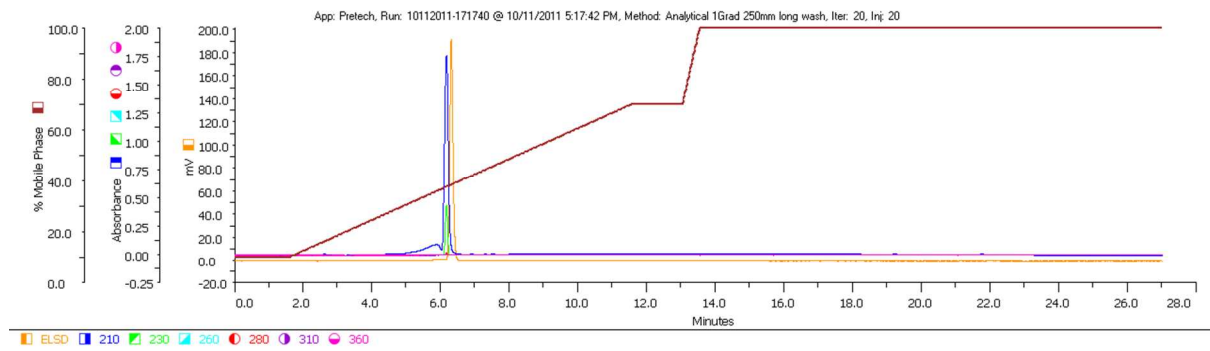
9 (AL039)



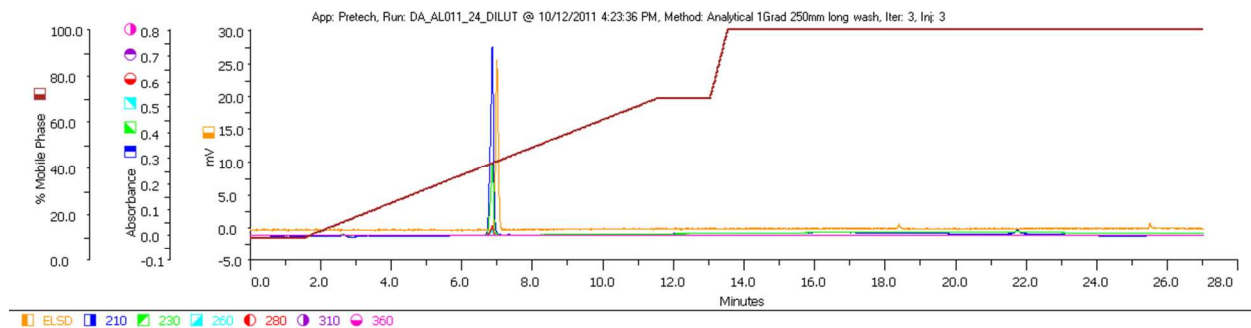
12 (AL040)



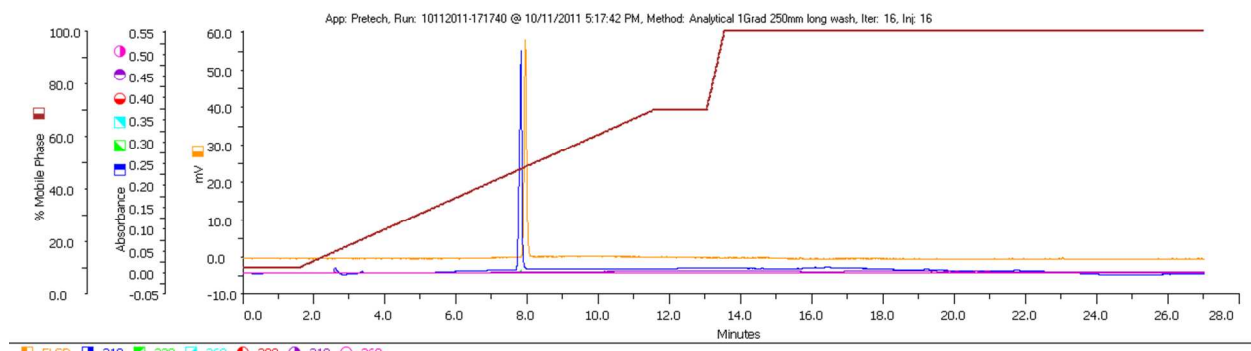
11 (AL041)



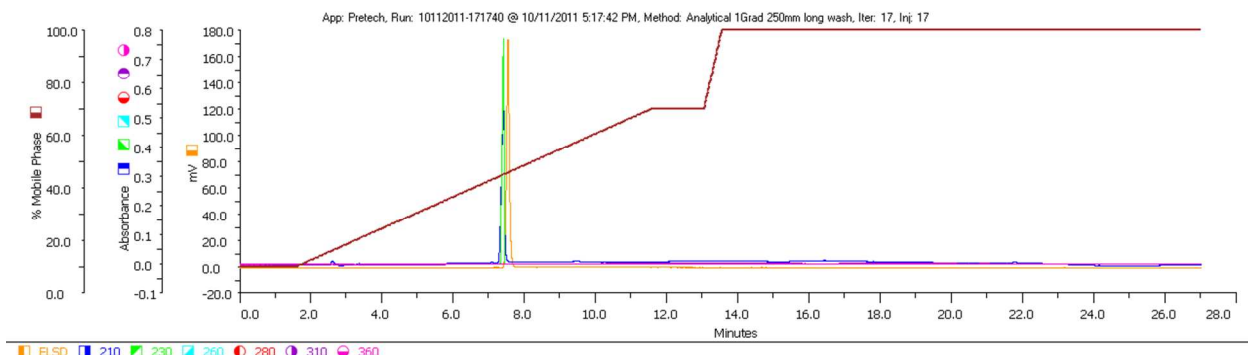
13 (AL024)



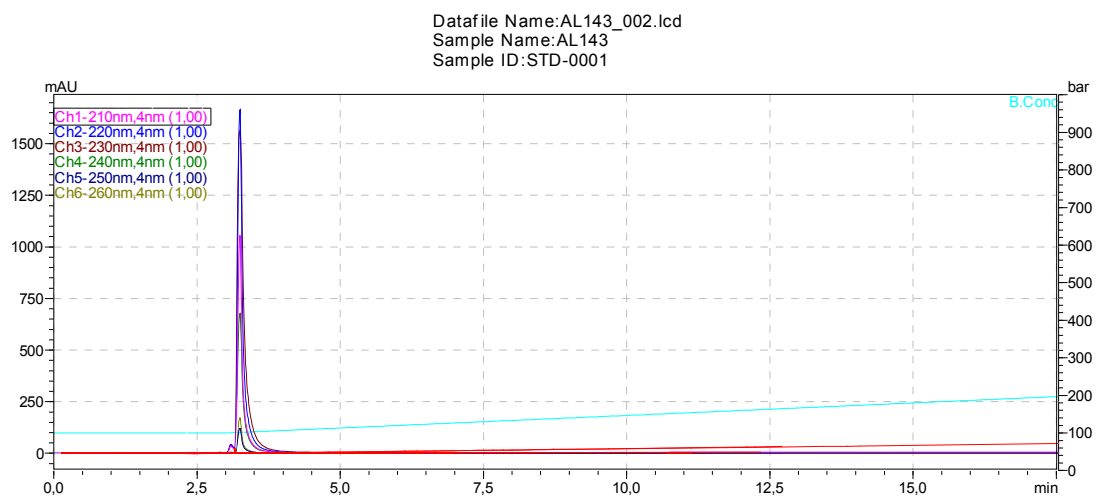
6 (AL037)



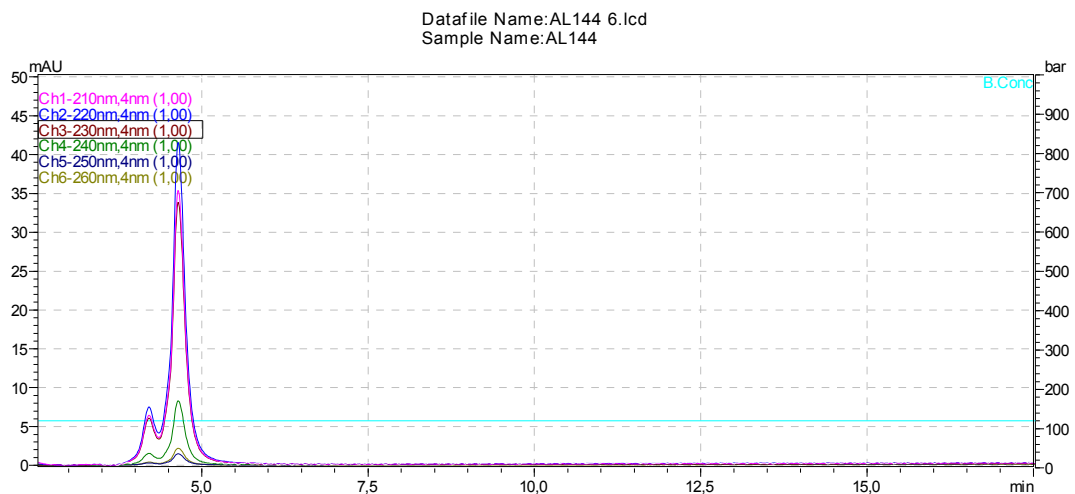
7 (AL038)



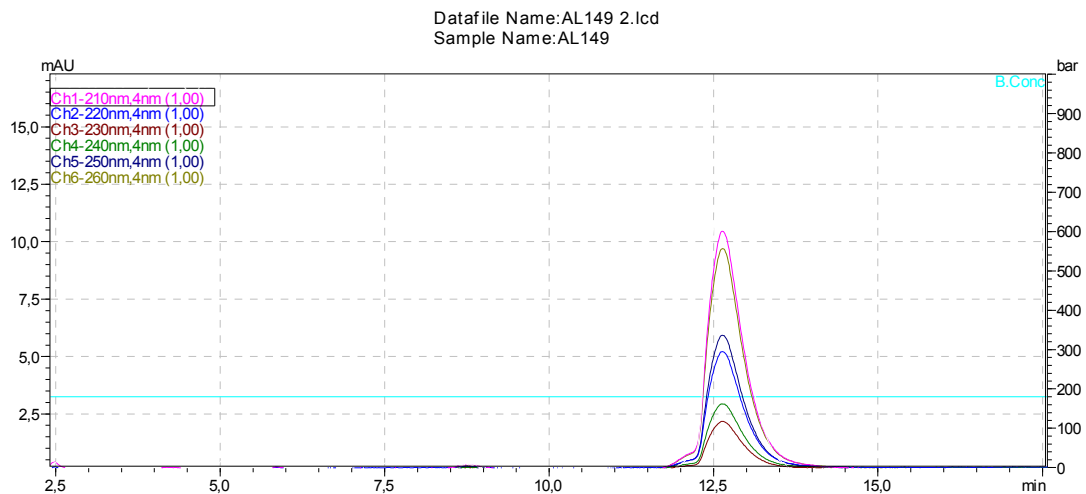
22 (AL143)



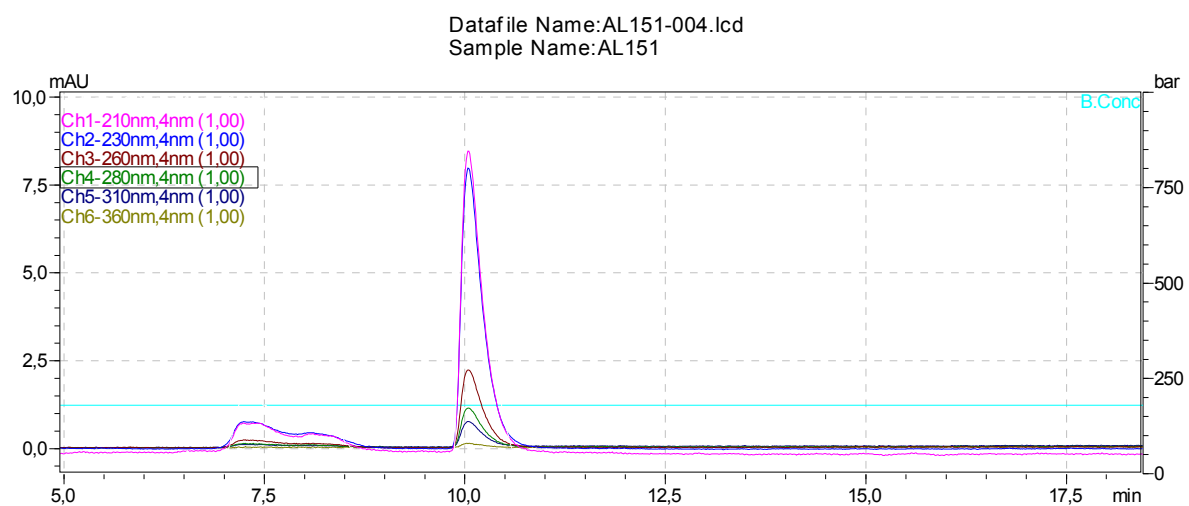
21 (AL144)



23 (AL149)



24 (AL151)



References

- (1) Brunger, A. T., Free *R* value: a novel statistical quantity for assessing the accuracy of crystal structures. *Nature* **1992**, *355*, 472-474.
- (2) Bourne, Y.; Taylor, P.; Radic, Z.; Marchot, P., Structural insights into ligand interactions at the acetylcholinesterase peripheral anionic site. *Embo J.* **2003**, *22*, 1-12.
- (3) MOE (*The Molecular Operating Environment*) 2011.10; Chemical Computing Group Inc., 1010 Sherbrooke Street West, Suite 910, Montreal, Canada H3A 2R7.
- (4) Kryger, G.; Silman, I.; Sussman, J. L., Structure of acetylcholinesterase complexed with E2020 (Aricept (R)): implications for the design of new anti-Alzheimer drugs. *Structure* **1999**, *7*, 297-307.